

FINAL REPORT

ASHRAE RESEARCH PROJECT

HEAT TRANSFER THROUGH ROLL-UP DOORS, REVOLVING DOORS AND OPAQUE NONRESIDENTIAL SWINGING, SLIDING AND ROLLING DOORS (1236-RP)

Prepared for:

American Society for Heating, Refrigerating
and Air-Conditioning Engineers, Inc. (ASHRAE)
1791 Tullie Circle NE
Atlanta, GA
USA 30329-2305

Attention: Mr. Michael Vaughn
Director of Research

Project sponsored by
ASHRAE Technical Committee 04.05 Fenestration

Report Prepared by:

Alex McGowan
Levelton Consultants Ltd.
520 Dupplin Road
Victoria, BC
V8Z 1C1

with

Robert Jutras and Gilbert Riopel
Air-Ins Inc.
3270 Boulevard Lionel-Boulet
Varenes, QC J3X 1P7

Morgan Hanam
Enermodal Engineering Ltd.
650 Riverbend Drive
Kitchener, ON N2K 3S2

July, 2006

File: 503-042B

EXECUTIVE SUMMARY

This report outlines research conducted on several non-residential door products, to assess their air-leakage characteristics and thermal transmittance (U-factors) at representative sizes.

Seven base-case specimens were tested and simulated in this project:

1. A non-insulated sectional door at 3.05m x 3.05 m (10' x 10')
2. An insulated sectional door at 2.74m x 2.13m (9' x 7')
3. A 3-wing revolving door at 3.05 m x 3.05 m (10' x 10')
4. A 4-wing revolving door at 2.4 m x 2.1 m (8' x 7')
5. A metal coiling slat door at 3.05 m x 3.05 m (10' x 10')
6. A single emergency exit door with no glazing, at 914 m x 2030 mm (3' x 6'8")
7. An aircraft hangar / warehouse door at 3.05 m x 3.05 m (10' x 10')

Specimen types and sizes were chosen to be representative of their product type, based on a market survey conducted as part of this project.

The products were tested to measure their air leakage at various pressure differentials, and to measure their thermal transmittance (U-factor) in the absence of air leakage. Computer simulation was used to determine total-product U-factors under standardized conditions.

Comparison between test and simulation procedures shows agreement to within accepted NFRC criteria for “equivalence” for all specimens except #1 and #5 (i.e., the non-insulated products). These products appear to have suffered from the different approaches used in test and simulation methods to develop room-side film coefficients, which are the controlling thermal resistance for these products. The test and simulation methods should be harmonized in this regard, or the NFRC procedures cannot be used to evaluate non-insulated products.

Several recommendations are made to modify the NFRC test and simulation procedures, to address specific considerations related to the products evaluated in this research project. Specific language appropriate to the relevant NFRC Standards is included in this report.

Air-leakage characteristics of the product types evaluated in this study are presented as a series of exponential correlations, of the form $Q = C \delta P^n$.

The scope of the project was extended using simulation to generate U-factors for the products for which “equivalence” was achieved. The resulting U-factors are presented in tables for inclusion in the ASHRAE Handbook of Fundamentals.

TABLE OF CONTENTS

PAGE NO.

1.	BACKGROUND.....	1
2.	MARKET STUDY AND BASE-CASE PRODUCT SELECTION.....	2
2.1	ONE-PIECE GARAGE DOOR	2
2.2	SECTIONAL GARAGE DOOR	3
2.3	REVOLVING DOORS	4
2.4	METAL COILING SLAT DOORS.....	5
2.5	EMERGENCY EXIT DOORS.....	6
2.6	SLIDING WAREHOUSE DOORS	6
3.	METHODOLOGY	7
3.1	AIR LEAKAGE TESTING.....	7
3.2	U-FACTOR TESTING.....	7
3.3	SIMULATION.....	8
3.4	CFD MODELING	9
4.	PRODUCT-SPECIFIC RESULTS	11
4.1	UNINSULATED SECTIONAL GARAGE DOOR	11
4.1.1	<i>Air-leakage testing</i>	12
4.1.2	<i>U-factor testing</i>	12
4.1.3	<i>U-factor Simulation</i>	13
4.2	INSULATED SECTIONAL GARAGE DOOR.....	18
4.2.1	<i>Air-leakage testing</i>	19
4.2.2	<i>U-factor testing</i>	19
4.2.3	<i>U-factor Simulation</i>	20
4.3	THREE-WING REVOLVING DOOR	22
4.3.1	<i>Air-leakage testing</i>	22
4.3.2	<i>U-factor testing</i>	23
4.3.3	<i>U-factor Simulation</i>	24
4.4	FOUR-WING REVOLVING DOOR.....	27
4.4.1	<i>Air-leakage testing</i>	27
4.4.2	<i>U-factor testing</i>	28
4.4.3	<i>U-factor Simulation</i>	29
4.5	METAL COILING SLAT DOOR.....	30
4.5.1	<i>Air-leakage testing</i>	30
4.5.2	<i>U-factor testing</i>	30
4.5.3	<i>U-factor Simulation</i>	32
4.6	EMERGENCY EXIT DOOR.....	34
4.6.1	<i>Air-leakage testing</i>	34
4.6.2	<i>U-factor testing</i>	34
4.6.3	<i>U-factor Simulation</i>	35
4.7	AIRCRAFT HANGAR DOOR.....	36
4.7.1	<i>Air-leakage testing</i>	37
4.7.2	<i>U-factor testing</i>	37
4.7.3	<i>U-factor Simulation</i>	38
5.	EXPANSION OF SIMULATION RESULTS	39
5.1	ONE-PIECE AND SECTIONAL TILT-UP GARAGE DOORS	40
5.2	REVOLVING DOORS	42
5.3	EMERGENCY EXIT DOORS.....	43
5.4	AIRCRAFT HANGAR DOORS	44
6.	CONCLUSIONS AND RECOMMENDATIONS.....	45
	REFERENCES.....	47



APPENDICES

- APPENDIX A1 Test Results for Specimen #1 (Non-insulated sectional door)
- APPENDIX A2 Test Results for Specimen #1 (Non-insulated sectional door) – Method B
- APPENDIX A3 Simulation & Air-leakage Results for Specimen #1 (Non-insulated sectional door)

- APPENDIX B1 Test Results for Specimen #2 (Insulated sectional door) – Test #1
- APPENDIX B2 Test Results for Specimen #2 (Insulated sectional door) – Test #2
- APPENDIX B3 Simulation & Air-leakage Results for Specimen #2 (Insulated sectional door)

- APPENDIX C1 Test Results for Specimen #3 (Three-wing revolving door)
- APPENDIX C1B Test Results for Specimen #3 (Three-wing revolving door) – Method B
- APPENDIX C2 Simulation & Air-leakage Results for Specimen #3 (Three-wing revolving door)

- APPENDIX D1 Test Results for Specimen #4 (Four-wing revolving door)
- APPENDIX D2 Simulation & Air-leakage Results for Specimen #4 (Four-wing revolving door)

- APPENDIX E1 Test Results for Specimen #5 (Metal coiling slat-type door)
- APPENDIX E2 Simulation & Air-leakage Results for Specimen #5 (Metal coiling slat-type door)

- APPENDIX F1 Test Results for Specimen #6 (Emergency exit door)
- APPENDIX F2 Simulation & Air-leakage Results for Specimen #6 (Emergency exit door)

- APPENDIX G1 Test Results for Specimen #7 (Aircraft hangar / warehouse door)
- APPENDIX G1B Test Results for Specimen #7 (Aircraft hangar / warehouse door) – Method B
- APPENDIX G2 Simulation & Air-leakage Results for Specimen #7 (Aircraft hangar door)

ACKNOWLEDGEMENTS

The 1236-RP project team (Levelton Consultants Ltd., Air-Ins Inc., and Enermodal Engineering Limited) would like to acknowledge the participation of the following sponsors, who donated products for testing and in some cases paid for shipping and customs brokerage:

- Boon Edam Corporation, Salt Lake City, UT
- C J Rush Industries Ltd., Markham, ON
- De la Fontaine Doors, Buckingham, QC
- Garaga Industries Ltd., St. Georges, QC
- Overhead Door Corporation, Dallas, TX
- Steel-Craft Door Products Ltd., Edmonton, AB
- A T Spec-Dor, Candiac, QC

We would also like to express our appreciation for the sponsorship of ASHRAE Technical Committee 4.5 (Fenestration), and for the guidance and collaboration of the TC4.5 Project Monitoring Subcommittee, without whom this project could not have been completed successfully:

- Jeff Baker, WESTLab, London, ON
- Dr. D.C. Curcija, University of Massachusetts at Amherst, MA
- Marcia Falke, Keystone Certifications, Inc., York, PA
- Joseph R. Hetzel, DASMA International, Cleveland, OH
- John Hogan (Chair), City of Seattle Dept. of Planning and Development, Seattle, WA

We also gratefully acknowledge the financial support of ASHRAE, Inc., and its generous donors, whose contributions enable projects such as this one to succeed.

1. BACKGROUND

ASHRAE provides design values for heat-loss coefficients for many different types of fenestration systems in Chapter 30 of the Handbook of Fundamentals (HOF; ASHRAE, 2001a). These tables include total-product U-factors for a wide range of planar window systems, but the information for doors is much more limited. Table 6 in the HOF gives a reasonable range of values for standard residential entrance doors, but only two values for revolving doors (one for the open position, one for closed), and only three values for different types of garage doors. The accompanying text notes that the values given “are generic values, and product-specific values determined in accordance with standards should be used whenever available.” This is better than no information at all, but leaves HOF users with little guidance, as the most widely cited national standard for thermal performance of doors in the United States is NFRC 100 (NFRC, 2004a), and that standard does not address revolving doors or many types of garage and rolling doors.

Table 6 in the HOF does not allow for the variation in thermal performance for product size, nor is any guidance given for variation in thermal performance due to different construction materials. For example, variations in the type of foam used in insulated-core doors is not addressed, and standard residential garage doors made of wood are not included in the HOF. The text accompanying Table 6 notes “a wide range in the design of insulated garage doors. Factors affecting heat transfer include width of insulation, thermal break design (if any), and design of interior skin.” No other guidance is given to the designer attempting to determine building-shell heat loss for entrance and egress systems.

The thermal performance of emergency-exit doors and large rolling or sliding cargo doors is not considered at all in the current HOF.

In response to the needs expressed by its members and the HVAC community, ASHRAE issued a request for proposal with the following objectives:

- Updating the information in Chapter 30 of the HOF to include more door types;
- Developing correlations to characterize convective flow and related heat transfer in enclosed chambers of revolving doors, for simplified calculation procedures.
- Evaluating the variation in thermal performance as a function of temperature conditions and product size; and
- Development of recommendations for testing and simulation of various door products, to provide guidance to designers for evaluation of products not in the current scope of work, and to assist in the development of national standards to evaluate such products.

This report describes research activities intended to achieve the above objectives.

The project was divided into six tasks, as described in the following sections of this report:

1. identify and acquire representative products
2. test base-case specimens (representative of the products identified in Task 1)
3. perform CFD simulation of convective motion in revolving doors
4. perform simplified 2D modeling of tested specimens
5. compare test and simulation results (develop modified methods if necessary)
6. expand scope of test results, using validated (or calibrated) simulation models

2. MARKET STUDY AND BASE-CASE PRODUCT SELECTION

A market study was undertaken to:

- characterize the various types of sliding and revolving doors
- identify typical construction materials
- determine the range of available product sizes
- develop a list of products for review and comment by the PMS
- select a set of specimens proposed for testing and simulation, for PMS review

The intent was to ensure that products evaluated in this project are representative of those available on the market. The market study entailed a review of supplier catalogues, industry catalogues (e.g., Sweet's, Fraser's), and manufacturers' Web sites, many of which can be found on Web sites for their trade associations (e.g., www.dasma.com, www.cdi-door.com).

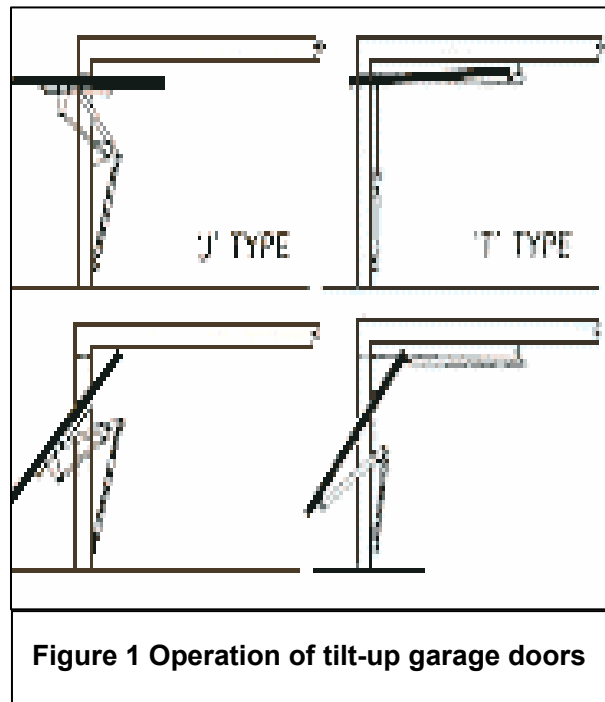
The project scope of work identified four product types: one-piece and sectional garage doors; metal coiling slat and rolling sheet steel doors; revolving doors; swinging steel emergency doors; and horizontal sliding cargo doors. Sections 2.1 – 2.6 describe these door types.

2.1 ONE-PIECE GARAGE DOOR

Also called a tilt-up door, a single-panel door, a canopy door, or (in the UK) an “up-and-over” door, this product comprises one-piece construction that pivots up toward the ceiling of the garage. Commonly constructed of wood or metal, but the metal product is (from a thermal perspective) a single layer of heavy-gauge steel. Thus, the only resistance to heat transfer is the room-side film coefficient. This product is included in the final project to provide a complete set of data, but inclusion of this or any products does not imply an endorsement (or condemnation) of the products in this study.

A one-piece wooden garage door is usually constructed as a stile-and-rail door. There are two operator types, depending on the mounting hardware used. Type 'J' doors pivot from jamb-mounted hardware. When the door is fully open, the door panel protrudes outside the garage (see Figure 1). In Type 'T' doors, the door panel runs on a track below the ceiling. When Type 'T' doors are open, the door panel sits almost entirely inside the garage. The Type 'T' door provides better air-sealing sealing over the 'J' type, but both doors require a gap around the full perimeter of the door panel for proper operation, and tend to have a higher rate of air leakage than sectional doors (see Section 2.2).

Some manufacturers will build one-piece custom doors on request. Common sizes include 2.44 m x 2.13 m (8' x 7'), 2.74 m x 2.13 m (9' x 7') and 4.88 m x 2.13 m (16' x 7'). This is not a common door, so it was not considered a typical baseline product, and a specimen was not tested as part of the scope of this project.



2.2 SECTIONAL GARAGE DOOR

As the name implies, a sectional door is constructed of individual sections, typically 4 or more. The sections are typically between 300 mm (1') and 600 mm (2') high, and the full width of the door. These sections articulate with each other to allow the door to open vertically on metal roller tracks. A sectional door is often preferred over a one-piece door (see Section 2.1) because:

- It is easier to operate;
- It does not restrict headroom in the garage as much as a one-piece door; and
- It requires almost no operating clearance (so that it can be opened even when a car is parked directly in front of it).

The door panels are typically 25 mm (1") or 35 mm (1-3/8") thick, with the latter being more common. Where manufacturers offer a range of sizes, these are typically widths of 2.4 m, 2.7 m, 3 m, 3.7 m, 4.3 m, 4.9 m or 5.5 m (8', 9', 10', 12', 14', 16' or 18') for residential products. Commercial products are also available in widths of 6.1 m, 6.7 m or 7.3 m (20', 22' or 24'). Door heights are typically 2 m, 2.1 m, 2.4 m or 3 m (6½', 7', 8' or 10') for residential doors, and from 2.1 m to 4.9 m in 300-mm increments (8' to 16' in one-foot increments) for commercial doors.

Of this range of sizes, the *most common* widths are 2.4 m or 2.7 m (8' or 9') for single doors and 4.9 m (16') for double doors, at either 2.1 m or 2.4 m (7' or 8') height for residential applications, and 3 m or 4.3 m (10' or 14') height for commercial buildings. The garage doors tested in this project were a non-insulated sectional door at 3.05 m x 3.05 m (10' x 10'), and an insulated sectional door at 2.74 m x 2.13 m (9' x 7').

Garage doors are made from wood, steel, aluminum, fiberglass or vinyl. Though each of these has its benefits, wood and steel garage doors are by far the favorites. **Wood** is preferred more for appearance than for durability. Wood is not as dimensionally stable as most other materials (it expands and contracts with changes in moisture content as well as with temperature). It is also more susceptible to weather damage, so regular maintenance (repainting, staining or refinishing every 2-3 years) is required. Wood flush-panel doors are usually finished with plywood, but raised-panel or recessed-panel construction is also common. Non-flush doors are typically rail-and-stile construction (similar to a swinging entrance panel door). Raised-panel profiles can be achieved with plant-on trim, whereas recessed-panel profiles are usually tongued panels fitted into a grooved softwood framework.

Steel provides the most durability of all materials used. **Aluminum** is more commonly used in one-piece, because it provides a lightweight panel that is easy to operate.

All metal doors are either single- or double-skin. Single-skin doors have an exterior metal facing and are either open at the back or feature a kraft-paper backing. They may or may not have insulated cores, depending on the climate: insulation is usually expanded polystyrene, foamed-in-place polyurethane, or polyisocyanurate. Some cores are of honeycombed cardboard, but this is becoming less common. Double-skin doors have a metal facing and a PVC, ABS or metal backing. The most common double-skin metal door has a steel facing and steel backing, and may incorporate a thermal break between the two metal layers. The thermal break typically provides a thermal separation on the order of 2 - 3 mm (1/10" to 1/8"), which would only be considered "thermally improved" in a window-frame design. It is possible that a larger thermal break cannot be provided due to the larger stresses in a larger operable product (i.e., a door panel), but for whatever reason a significant thermal break is the exception in door design. The largest thermal break we found in our market research was in one product with a 9 mm (3/8") vinyl thermal break, but this product was not rated for fire resistance (presumably, the vinyl would not withstand the heat of a fire). A "thermally broken" (thermally improved) double-skin door with an insulated core is common, and was one of the products we selected for testing with respect to this project.

Lightweight steel and aluminum doors are susceptible to impact damage, and a minimum of 26-gauge metal is common for the front facings. The backing is less prone to impact, and can be of any thickness.

Fiberglass doors are actually an aluminum or steel structure covered with fiberglass to reduce weight. **Vinyl** doors are similar in construction. Both may be designed to be resistant to salt-air corrosion. The majority of sectional doors appear to be steel-skin, however, especially in commercial applications. Wood garage doors are available, but almost entirely in the residential market: we estimate wooden sectional doors to be less than 5% of the commercial market.

Two specimens were selected as representative of sectional garage doors. Both are steel-skin doors, representing the majority of doors of this type. One specimen is a “single-skin” door with no insulation, commonly used in the southern United States, and one is a “double-skin” door with steel panels (separated by a thermal break) on either side of an insulated core. The latter is commonly used in the northern United States and in Canada, and is available with several different types of insulation. The product chosen was filled with polyurethane foam (nominal center-of-panel thermal resistance of $2.83 \text{ m}^2\text{C/W}$, or $16 \text{ hr}\cdot\text{ft}^2\cdot^\circ\text{F/BTU}$).

Assuming we could achieve reasonably good agreement between test and simulation for the sectional garage-door products, it was proposed to derive values for one-piece door products (see Section 2.1) using simulation only.

2.3 REVOLVING DOORS

These are the most complex of the products to be evaluated in this project. The assembly includes a barrel or cylinder, inside of which is a set of radially arranged panels that rotate around a vertical axis at the center of the barrel. Revolving doors in applications where the passage of large items are anticipated (e.g., hospital gurneys at hospitals or luggage carts at airports) usually have only two door panels, but three-, four-, and five-panel doors are more typical. The most common is the four-panel door, with the three-panel as a distant second choice. Figure 2 shows the two-, three-, and four-wing configurations with the door in the “closed” position.

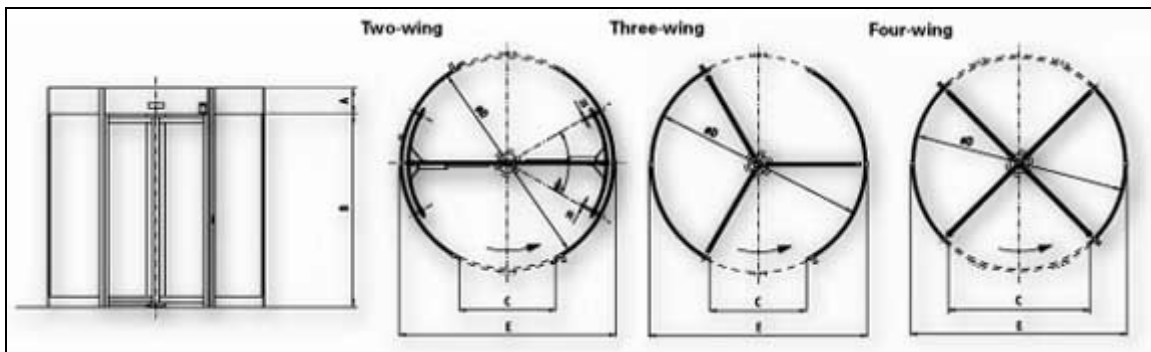


Figure 2 Elevation and plan views of 2-wing, 3-wing and 4-wing revolving doors

This door type is often promoted as energy-efficient, due to the lower air-leakage characteristics as compared with other entrance systems. The configuration of the assembly, however, is such that the surface area of the barrel is much greater than an equivalent planar entrance system, and the projecting roof of the revolving door further increases the surface area exposed to the exterior and the conditioned space. The total heat transfer through this assembly should therefore be expected to be greater than a planar entrance system installed in the same rough opening in the wall, by at least the ratio of surface area to projected area of the opening.

The door panels are almost always metal and glass, and can be constructed in a stile-and-rail assembly or as glass panels (see Figure 3 at right). Typical sizes are 2.1 m or 2.4 m (7' or 8') in diameter, and 1.8 m, 2 m or 2.1 m (6', 6½', or 7') height. Larger sizes are possible, especially for the 2-wing or 3-wing models.



Figure 3 Typical four-wing revolving-door

Two revolving door specimens were selected for analysis in this project: a 3-wing door at 3 m x 3 m (10' x 10'), and a 4-wing door at 2.4 m x 2.1 m (8' x 7'). The four-wing door is somewhat similar to the product shown in Figure 3. Specific products tested are described in greater detail in Section 4.

2.4 METAL COILING SLAT DOORS

Also known as roll-up doors, these products are large doors that open by sliding vertically to roll around a capstan at the top of the opening (see Figure 4). The facing is steel (other types of doors are rare), at a minimum thickness of 22 gauge. These doors may be insulated or non-insulated, depending on the application.



Figure 4 Typical metal coiling slat door

These doors are built for almost any size opening, but common sizes are 2.4 m x 2.4 m, 3 m x 3 m, or 4.3 m x 4.3 m (8' x 8', 10' x 10', or 14' x 14').

There are two types of metal coiling doors. One comprises a single sheet of patterned steel with reinforcing straps. The other, more common, construction is a slat-type roll-up door in a metal frame. The latter is more durable, as the sheet-steel door is more likely to exhibit fatigue cracking over time.

The metal coiling slat door is similar in concept to the sectional garage door (see Section 2.2), except the height of the “panels” (slats, in this case) is typically only 64 mm or 65 mm (2-1/2” or 2-9/16”). The slats themselves can be unbacked, or backed with plastic or fabric backing (see Figure 5) to provide an interior finish and some increase in thermal resistance.

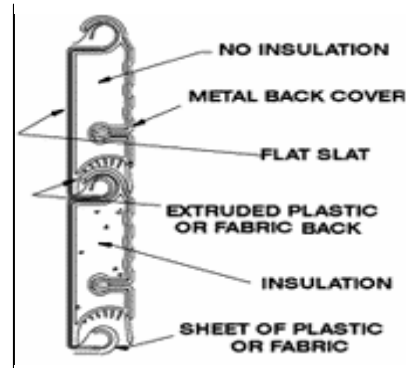


Figure 5 Metal coiling door slats may be insulated

The product selected for this project was a non-insulated metal coiling slat door at a test size of 3 m x 3 m (10' x 10'). Assuming that reasonably good agreement between test and simulation results could be achieved, it was the intention to use simulation to produce values for insulated doors (and for insulated and non-insulated doors at various sizes).

2.5 EMERGENCY EXIT DOORS

These doors are required by building codes in most jurisdictions to provide egress in case of emergency. Because of the requirement for continued fire protection while occupants escape during an emergency, almost all of these products feature double steel skin (i.e., a sheet steel layer on interior and exterior surfaces), which is usually separated by an insulated core. Typical insulation options include polyurethane foam, rigid polystyrene foam, semi-rigid glass-fiber insulation, or honeycombed corrugated paper.

Most emergency exit doors are opaque, but some have small glazed panels (see Figure 6), and some are half-glazed (i.e., the upper half is a glazed panel). The glass panels in these glazed products are usually reinforced with steel wire to minimize breakage during a fire.



Figure 6 Emergency exit door

As these doors are standardized products, the sizes show little variation. Door heights are either 2 m or 2.4 m (6'8" or 8'), and widths are 914 mm (3') for a single door, or 1.8 m (6') for a double door, as shown in Figure 6. As was discussed with garage doors (see Section 2.1), most emergency exit doors have a minimal thermal break, or none at all.

The test specimen was a single door with no glazing, at a size of 914 mm x 2030 mm (3' x 6'8"), installed in a steel frame.

2.6 SLIDING WAREHOUSE DOORS

This is typical of doors for aircraft hangars and large production facilities or warehouses. Individual door panels are constructed from a tubular steel frame, with infill construction to match the wall assembly of the building. Profiled steel is typically the exterior cladding, but a wide range of finish materials are available, and door assemblies are usually engineered to suit a specific application. Therefore, almost all of these assemblies are custom-built, and the cost of engineering design is included in the product cost.



Figure 7 Typical aircraft hangar door

The panels roll on tracks or rollers at the base of the wall, or on overhead hangers in some types of construction.

The doors can be glazed (see Figure 7), but are more often opaque. As these assemblies are custom-built, they are available in any size. The sizes can be quite large, particularly in the application of aircraft hangars.

3. METHODOLOGY

3.1 AIR LEAKAGE TESTING

The products selected as base-case specimens were tested for air leakage. The test procedures followed the NFRC 400 protocol (NFRC, 2004d) as closely as possible, with some modification to allow testing of certain products. All tests were conducted at three different pressure differentials, namely 25, 50 and 75 Pascals (0.1, 0.2 and 0.3 inches of water). This allowed us to develop a simple polynomial to describe air leakage as a function of pressure difference, which could prove useful in load calculations or computational algorithms.

Some specimens were re-tested for air leakage characteristics using different weatherstripping accessories, according to the options provided by the manufacturers for that product type. The revolving doors were also tested in different operating configurations, to examine how the air-leakage characteristics of these assemblies vary with the position of the door panels.

3.2 U-FACTOR TESTING

All products were tested to determine thermal performance, as characterized by the heat loss coefficient (total-product U-factor). The test procedures followed the NFRC 102 (NFRC, 2004c) protocol as closely as possible, but some modification was required to allow testing of certain products. The revolving doors, for example, are much deeper than any other products tested in the NFRC 102 methodology (which was developed to evaluate planar products), and the hangar and roll-up doors are larger than the standard 2.4 m x 2.4 m (8' x 8') size referenced in that standard. The version of the NFRC standard in place when this testing was conducted did not reference the evaluation of garage doors using testing – the procedure is for simulation only – so some additional modification to the NFRC 102 protocols were necessary for this project.

Where possible, products were tested in accordance with the CTS method and with the area-weighting method, both described in ASTM C1199 (ASTM, 2000; the test protocol referenced in NFRC 102). The CTS method uses a control specimen of known conductance to determine the film coefficients for the test chamber, based on the concept that these film coefficients will be the same when the test specimen is installed in place of the Calibration Transfer Standard (CTS) panel. During the CTS calibration procedure, the air velocity of the weather-side wind is measured, and this velocity must be controlled in such a way as to produce a mean weather-side film coefficient of $30.0 \text{ W/m}^2\text{-K}$ ($5.28 \text{ BTU/hr-ft}^2\text{-}^\circ\text{F}$) $\pm 10\%$. This same air velocity is produced when the test specimen is installed, thus ensuring that the weather-side film coefficient is known.

The area-weighting method requires temperature measurements on the test product near the edges, center-of-panel, framing components and any other test-specimen surfaces. The temperatures obtained from these thermocouple measurements are assumed to represent the average temperature of the surface area upon which each thermocouple is centered, so these values are used to calculate the mean surface temperature on both sides of the specimen. Knowing the air temperatures on either side of the specimen, and the total heat transfer through the specimen, it becomes simple to calculate the film coefficient on either side of the specimen.

The accuracy of the area-weighting method depends on appropriate placement of the thermocouples, to ensure that the temperatures that are measured are truly representative of the average values for the product being evaluated. Wherever possible, we referred to specified thermocouple placements in similar product configurations (for example, the elevation view of a revolving door is similar to that of a patio door, except for the curved barrel extensions, so the thermocouple placement for those specimens is based on Figure 11-1 from NFRC 102.

Additional thermocouples were added in all cases to obtain information about thermal gradients near locations of interest (e.g., edges of panels, meeting rails, reinforcing elements, fasteners). All proposed thermocouple arrangements were submitted to the Project Monitors prior to testing, to ensure that the area-weighted approach would be valid, and that the most useful information would be captured in the testing of each specimen.

Whichever procedure is used to determine the film coefficients of the test specimen, these values are mathematically subtracted from the as-tested thermal transmittance (U-factor) of the specimen, and standardized film coefficients are added on to convert the as-tested transmittance, U_s , to a standardized U-factor, U_{st} . In this way, all products are evaluated under a standard set of conditions (i.e., the same film coefficients).

The specimens were sealed against air leakage during the U-factor testing, to avoid contaminating U-factor test results with air-leakage effects. This is in keeping with the NFRC 102 methodology, and with the design principle that treats air leakage and U-factor as entirely separate aspects of heating- and cooling-load calculation procedures.

3.3 SIMULATION

As in the case of testing, the simulation procedures used in this project follow those outlined in the NFRC 100 Standard as much as possible. Where this was not possible (e.g., there is no standardized procedure for simulating the performance of revolving doors), the underlying principles (described in Enermodal, 1996) were used to develop an appropriate strategy.

The baseline test specimens described in Section 2 were simulated using NFRC 100 procedures. Specifically, we created computer models of each component of each product, and area-weighted the component U-factors to determine a total-product U-factor:

$$U_t = (U_h * A_h + U_s * A_s + U_e * A_e + \dots) / (A_h + A_s + A_e + \dots), \quad <1>$$

where U is the component U-factor, and A is the associated projected area, of the head, sill, end-stile, etc., components, as denoted by the subscripts in equation <1>. Specific calculations are given for each specimen in the discussion of results in Section 4 of this report.

The scope of work for this project entailed testing and simulation of the thermal performance (total-product U-factor) of seven (7) specimens. For those products that showed acceptable agreement between test and simulated results, the project uses an appropriate level of simulation to generate additional U-factors for products similar to the base-case specimens. The products chosen for comparison of test and simulation results were selected to provide a reasonable level of confidence in our ability to characterize the thermal performance of that product and minor variations in its design (which would be evaluated using simulation). In any project of this nature, the methodology used to expand the scope of the results using simulation only should be such that the level of confidence in the simulation-only results is equal to or better than that of the simulated-and-tested results.

The specific nature of each of the seven specimens tested entailed specific assumptions and methods for testing and simulation. Therefore, each of these product-specific considerations is discussed in Section 4 of this report, along with the presentation of results for each specimen.

Note that, for the sake of brevity, only *departures* from existing standard procedures (e.g., NFRC 100, NFRC 400) are noted in this report. The reader is encouraged to review the Standard documents referenced herein for a complete description of the testing and simulation protocols followed during the normal course of this project.

3.4 CFD MODELING

The current version of NFRC 100 does not provide a method for determining the U-factor of a revolving door using calculation or computer simulation. Therefore, part of this project involved development of such a procedure. This procedure was developed following the general underlying philosophy behind the original NFRC simulation procedures. The Principal Investigator for this project was one of the chief authors of the original documentation (Enermodal, 1996) on which the NFRC simulation “rules” are based.

In the special case of a revolving door, the unusual configuration of the door type introduces more complexity to the simulation procedure. Natural-convection cells will develop inside the pie-shaped chamber formed between the closed door panels and the surrounding barrel (the barrel is formed by the curved panels that enclose the central revolving component). The computational software used in the NFRC procedures is a simplified two-dimensional program that does not explicitly model convective heat transfer. Rather, all components are modeled as solid components with a constant thermal conductivity. Increased heat transfer due to convective motion in a fluid can be modeled by assigning an “effective thermal conductivity” to the component. The difficulty is in knowing what value to assign to the conductivity that will properly account for convective heat transfer.

To solve this problem, an explicit three-dimensional model of the enclosed air chamber in the door was developed using a computational fluid dynamics (CFD) software program. The software models convective and radiative heat transfer, and can be used to examine characteristic heat flows for a range of geometries and boundary conditions. A CFD model of the door chamber and enclosing solid components (e.g., door glazing, aluminum framing elements) was run with typical room-side and weather-side boundary conditions to obtain overall heat flow (see Figures 8 and 9). Then the CFD model was run with a constant value of thermal conductivity for the door chamber, λ_{eff} . The value of λ_{eff} that produced the same heat flow rate as the explicit CFD model was considered to be the average effective thermal conductivity of the air cavity. This value was used in a simplified 2D model to obtain average heat flow (and thus the component U-factor) for all appropriate cross-sections, and is summarized in Table 1.

Assuming that this approach provided good agreement with the test results, however, we would be able to generate representative values for the effective thermal conductivity of enclosed air cavities using CFD runs for other configurations.

Table 1 Results of CFD Models for Revolving Door Specimens

Description	$T_{ia} / T_{oa}, ^\circ\text{C} (^\circ\text{F})$	Door radius, m (ft)	Conductive path mean length, m (ft)	Door Panel Area, m^2 (ft^2)	Heat flow from CFD model, W (BTU/hr)	$\lambda_{eff}, \text{W/m-K}$ (BTU-in/hr-ft ² -°F)
1.8 m x 1.8 m (6' x 6') 4-wing	21 / -18 (70 / 0)	0.91 (3)	1.09 (3.6)	1.67 (18)	285 (972)	1.57 (10.88)
2.1 m x 2 m (7' x 6½') 4-wing	10 / -29 (50 / -20)	1.07 (3.5)	1.28 (4.2)	2.11 (22.8)	353 (1204)	1.83 (12.69)
2.1 m x 2 m (7' x 6½') 4-wing	21 / -18 (70 / 0)	1.07 (3.5)	1.28 (4.2)	2.11 (22.8)	340 (1160)	1.74 (12.06)
2.1 m x 2 m (7' x 6½') 4-wing	35 / 24 (95 / 75)	1.07 (3.5)	1.28 (4.2)	2.11 (22.8)	59.5 (203)	1.07 (7.42)
2.4 m x 2.1 m (8' x 7') 4-wing	21 / -18 (70 / 0)	1.22 (4)	1.46 (4.8)	2.6 (28)	445 (1518)	2.11 (14.63)
2.4 m x 2.1 m (8' x 7') 3-wing	21 / -18 (70 / 0)	1.22 (4)	1.34 (4.41)	2.6 (28)	464 (1583)	2.37 (16.43)
3 m x 3 m (10' x 10') 3-wing	21 / -18 (70 / 0)	1.52 (5)	1.68 (5.51)	4.64 (50)	711 (2426)	2.55 (17.68)

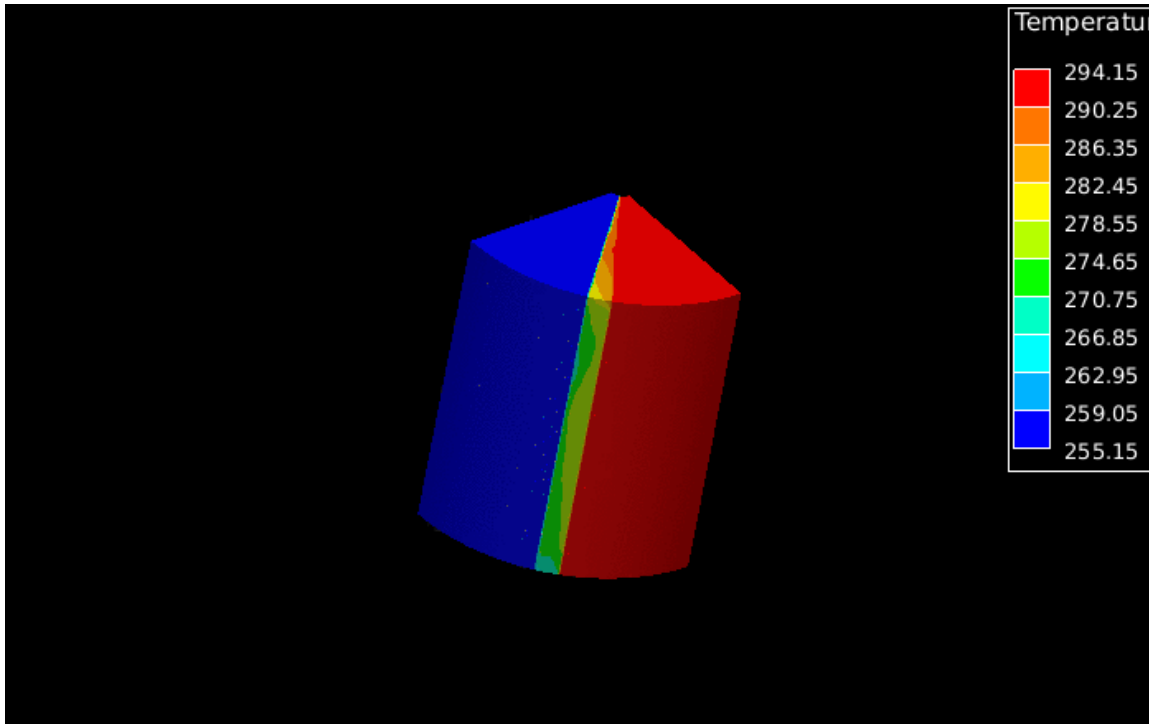


Figure 8 Temperature Profile of 4-wing door CFD model (boundary conditions)

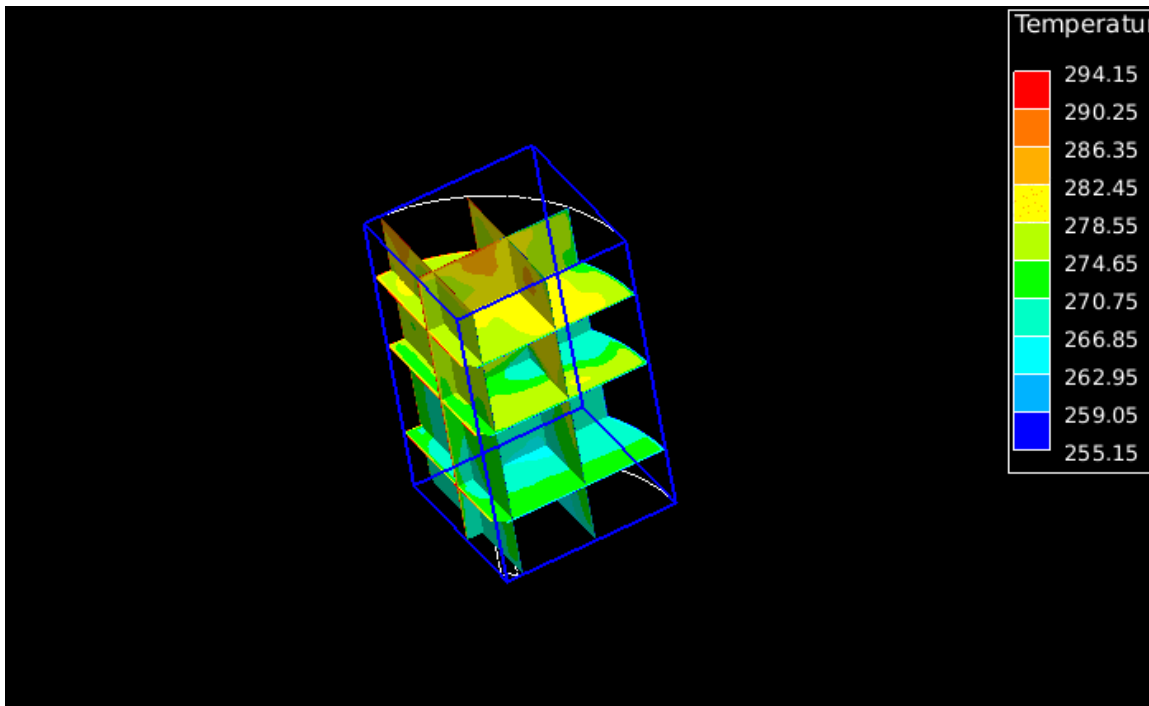


Figure 9 Temperature Profile of 4-wing door CFD model (internal sections)

4. PRODUCT-SPECIFIC RESULTS

4.1 UNINSULATED SECTIONAL GARAGE DOOR

This specimen was a steel sectional garage door manufactured by Steel-Craft Door Products Ltd. (see Figure 10). The door sections were nominally 50 mm (2") overall thickness, constructed of 24-gauge roll-formed commercial quality ZF075 Galvaneal steel. Meeting rails were rabbeted to form a weather seal (but not an air seal) between sections. Each of the five sections the door assembly was reinforced with two steel ribs, with end channels wrapped around each section and spot-welded in place.

Galvanized hardware provided with the door included adjustable top roller brackets, end-roller and intermediate hinges, and galvanized steel door tracks on either side, to represent typical installation.

The door tracks normally extend along the ceiling a garage, to guide the door sections as the assembly opens, but the tracks in the test specimen had to be cut at the top of the door, to avoid interference with the constant-temperature baffle and the convective flow of room-side air during the thermal testing. Figure 11 shows this procedure for Specimen #2, but Specimen #1 was installed in the same way.

The bottom of the door included a weather seal made of a U-shaped extruded vinyl bulb seal, typical of this type of installation. Perimeter seals the jambs and head of the door assembly are optional accessories, but are often not installed as they may interfere with door operation. The perimeter seals were not installed in this specimen.

The specimen is shown in Figure 10 installed in the mask wall, and was moved with the mask wall from the air-leakage test chamber to the thermal test chamber as a unit. The rigid polystyrene-foam panels shown inside each door section were for shipping purposes only, and were removed prior to testing for air leakage and U-factor.



Figure 10 Specimen #1 Non-insulated Sectional Garage Door (rigid insulation in door panels was removed before test)



Figure 11 Door track cut to fit assembly into test chamber (for Specimen #1 and #2)

4.1.1 Air-leakage testing

The non-insulated garage door was tested for air leakage following NFRC 400 procedures. The existing Standard can be used for these products, except that we did not record the operating forces to initiate and maintain motion, per the Standard, as it was not within the scope of the ASHRAE project. Recording operating force is done in NFRC evaluations to ensure that a manufacturer is not artificially enhancing the air-leakage test by applying larger seals than are necessary (which would interfere with the operation of the product). That consideration does not apply in this case, because the opposite is typically true of the types of products evaluated in this study (the weatherstripping is intentionally loose to permit free operation of the door assembly).

The air-leakage test results for the non-insulated sectional door are shown in Appendix A. The results show good agreement with the classic formulation of air-leakage models, $Q = C \delta P^{0.65}$. Our analysis has determined that, for the specimen tested, air leakage varies with applied air pressure according to:

$Q = 0.163 \delta P^{0.65}$, where Q is air leakage in L/s per m² and δP is air-pressure difference in Pa (or $Q = 1.16 \delta P^{0.65}$, if Q is measured in cfm per ft² and δP is measured in inches of water).

At 75 Pa pressure difference (the standard criterion for NFRC 400), the air leakage for this product was measured to be 2.65 L/s per m² of projected area (0.52 cfm per ft²). To provide context, this can be compared with a code-based requirement for swinging doors, which specifies a maximum air leakage of 1.88 L/s per m² (0.37 cfm per ft²). In that context, the air leakage for this specimen was approximately 50% greater than an equivalent swinging door. It should be recognized that, like the other specimens in this study, the primary purpose of these assemblies is the control of building access, and not necessarily airtightness or energy efficiency.

4.1.2 U-factor testing

The non-insulated sectional door was tested in accordance with NFRC 102. The recommended size for testing garage doors (per NFRC 102) is 3 m x 2.39 m (118" x 94") or larger, unless the test chamber cannot accommodate this size (in which case 2.44 m x 2.44 m, or 96" x 96", is specified as the appropriate size). The product tested was 3.05 m x 3.05 m (10' x 10'), which is the rough opening size. The test product is slightly larger, due to the door frame (see Figure 10), but the frame would not be included in the overall U-factor calculation in a load calculation, and therefore was not included in these test results.

The results of U-factor testing of this product are shown in Appendix A, which also includes photographs of the products with thermocouple readings superimposed on the images to indicate the as-tested temperature distribution on both side of the specimen. For this specimen, the results are:

Table 2 Specimen #1 Test Results

As-tested	Area-weighting method					CTS method				
U_s	T_{is}	h_i	T_{os}	h_o	U_{stA}	T_{is}	h_i	T_{os}	h_o	U_{stB}
6.23 (1.10)	-2.65 (27.2)	10.21 (1.80)	-3.65 (25.4)	17.28 (3.04)	5.43 (0.96)	-3.75 (25.2)	9.72 (1.71)	-8.80 (16.2)	27.05 (4.76)	4.94 (0.87)

Note: Temperatures t_i and t_o in °C (°F), U-factors and film coefficients h_i and h_o in W/m²-K (BTU/hr-ft²-°F)

The difference between the results for the area-weighting and CTS methods is due to the surface temperatures predicted by the different methods. The area-weighting method predicts a nearly isothermal specimen (i.e., $t_i \approx t_o$), as one would expect for a product that is essentially a single layer of metal. The CTS method, however, predicts a temperature difference of over 5 C° (or 9 F°) between

the interior and exterior surfaces of the specimen, which is not consistent with what one would expect for a non-insulated specimen. A review of the data for the thermocouple pairs installed on either side of the specimen (see Appendix A) favors the near-isothermal case, so we recommend that the area-weighting method should be used for this specimen. This is consistent with ASTM C1199, which specifies that the area-weighting method is to be used for specimens where $U_s > 3.4 \text{ W/m}^2\text{-K}$ ($0.6 \text{ BTU/hr-ft}^2\text{-}^\circ\text{F}$), or if the ratio of projected area to surface area is less than 0.80. It is not consistent with the current version of NFRC 100, which specifies that all products are to be evaluated using the CTS method.

We recommend that ASTM C1199 should be followed regarding area-weighting vs. CTS methods for high-conductance specimens ($U_s > 3.4 \text{ W/m}^2\text{-K}$ or $0.6 \text{ BTU/hr-ft}^2\text{-}^\circ\text{F}$).

Specific Standards Language: NFRC 102 contains a clause 8.2 that modifies ASTM C1199 to require the CTS method to be used for all products. This does not appear to be appropriate for high-conductance products.

We recommend that Clause 8.2 in NFRC 102 should be deleted.

The measured surface temperatures for this product (see Appendix A) appear to indicate a temperature stratification at the warm surface, with the top of the door approximately 8°C (14°F) warmer than the bottom. This is consistent with the development of a boundary layer on that surface, and suggests a higher rate of heat loss at the top of the door than at the bottom.

4.1.3 U-factor Simulation

The simulation models used to represent this product, and the resulting component and area-weighted U-factors, are shown in Appendix A. The first simulation produced a total-product U-factor of $4.39 \text{ W/m}^2\text{-K}$ ($0.77 \text{ BTU/hr-ft}^2\text{-}^\circ\text{F}$), well below the tested values (U_s or U_{st}), which indicated that the simulation model was not accounting for all of the heat transfer in the test specimen. The standard NFRC procedure for modeling sectional doors includes 63.5 mm ($2.5''$) of edge-of-panel in the model, and it was conjectured that this might not capture all of the heat flow in a steel-skinned product (where the skin of the non-insulated door panel acts like a fin). When we increased the height of the edge-of-panel portion in the model, we observed an increased in the U-factor, but increasing the edge dimension beyond 150 mm ($6''$) produced a negligible increase in the result. We therefore determined that the larger edge dimension was necessary in this model, to account for all of the heat transfer in the as-tested specimen.

We recommend including a larger portion of edge-of-panel in the 2D model for this type of product. It requires little additional effort to create the model, and greatly improves the accuracy of the result.

Specific Standards Language: where Figure 5-13 in NFRC 100-2004 indicates that the edge-of-panel area is 63.5 mm ($2.5''$), this should be changed for products with significant edge effects. The technically correct methodology, as was used in this project, is to incrementally increase the edge-of-panel height until subsequent iterations produce no change in the result, but this may not be desirable language in a Standard such as NFRC 100. It may be adequate to simply replace the 63.5 mm ($2.5''$) dimension in Figure 5-13 with the 150 mm ($6''$) dimension developed in this study, but there is no guarantee that this would be suitable for all products.

We recommend modifying Figure 5-13 in NFRC 100 so that the “edge-of-panel area” reads 150 mm ($6''$) instead of 63.5 mm ($2.5''$) – or so that it reads “Edge-of-Panel Area: height varies”, with a direction in the Simulation Manual to incrementally increase edge-of-panel height until subsequent iterations produce no change in the result.

When we calculated the total-product U-factor with a 150-mm (6") edge, the result was 4.84 W/m²-K (0.85 BTU/hr-ft²-°F). At that point in the project, the test and simulation results agreed to within 12.1% (for Method A of the test) or 2.1% (for Method B). As we are of the opinion that Method A is more accurate, the results do not meet the validation criterion of the NFRC 100 procedure (NFRC requires agreement to within 10%). Having exhausted all other possible reasons for the lack of agreement, the test and simulation laboratories were allowed to discuss the results in an attempt to resolve the discrepancy. It became apparent that the simulation assumption of a galvanized surface was incorrect, as the testing laboratory verified that the surface was coated with a primer. The primer-coat mimicked the dull gray finish of a galvanized surface, and it was only evident on close visual inspection that the surface was painted.

The simulation results were recalculated using a painted surface, which changes the surface emittance from 0.90 to 0.20. The resulting U-factor was 6.72 W/m²-K (1.18 BTU/hr-ft²-°F), which is well beyond the NFRC agreement criterion. To examine the reasons for this difference, the project team looked at the simulation results. Specifically, the total-product thermal transmittance (as predicted by simulation) was separated into the specimen conductance and room-side and weather-side film coefficients.

Unfortunately, THERM (LBNL, 2003); the software used to determine total-product U-factors via computer simulation) does not provide explicit values for the total room-side film coefficient, so the value must be backed out of the results. Consider an energy balance on the specimen: the heat flow from the room to the specimen can be expressed as $Q = h_{is} * A_s * (T_{ia} - T_{is})$, and the overall heat transmission through the specimen is $Q = U * A_p * (T_{ia} - T_{oa})$. Equating these flows, we get $h_{is} * A_s * (T_{ia} - T_{is}) = U * A_p * (T_{ia} - T_{oa})$, and solving for the total room-side film coefficient:

$$h_{is} = U * \frac{(T_{ia} - T_{oa}) * A_p}{(T_{ia} - T_{is}) * A_s} \quad <2>$$

where U is the total-product U-factor, either from test or simulation;
 T_{ia} , T_{oa} and T_{is} are the temperatures of the indoor and outdoor air, and indoor surface; and
 A_p and A_s are the projected and actual wetted surface areas of the specimen

A similar derivation can be used to produce the exterior film coefficient, but the value of interest is on the room side, as this is the controlling resistance of the non-insulated specimen. Most of the above variables are easily obtained: from the physical configuration of the specimen (A_p and A_s) or the specified boundary conditions (T_{ia} and T_{oa}). The U-factor is produced from the simulation, and it only remains to obtain a mean surface temperature for the corresponding U-factor. Unfortunately, THERM does not make this easy, especially where the interior surface is irregular. To obtain an approximation of this value, we took advantage of the physics of the situation. As this is a high-conductance specimen that is nearly isothermal, according to the thermocouple readings from the test (see Appendix A) and the preliminary simulation results, we made the approximation that the room-side surface temperature is equal to the weather-side surface temperature (i.e., $T_{is} \approx T_{os}$). This approximation is seen to be intuitively true for most of the specimen, as it is essentially a single layer of 24-gauge galvanized steel (except at joints between slats, and at the perimeter of the specimen), as shown in Appendix A. To simplify our analysis, we focused on the center-of-panel, which comprises two-thirds of the specimen's area. This allows us to approximate the room-side film coefficient without the geometric complications that occur at the perimeter of the specimen (including the mounting track and mask-wall interface). The convective portion of the room-side film coefficient is assumed in THERM to be constant for a given type of frame, so the radiative component can also be isolated.

The room-side film coefficient is determined in the test according to Clause 8.2.9.1 of NFRC 102:

$$h_{STh} = 1.46 \left[\frac{(T_{ia} - T_{is})}{H} \right]^{0.25} + \sigma \varepsilon_1 \frac{[(T_{ia} + 273.16)^4 - (T_{is} + 273.16)^4]}{(T_{ia} - T_{is})} \quad <3>$$

where H is the height of the specimen;
 σ is the Stefan-Boltzmann constant; and
 ε is the mean surface emittance of the specimen

It is interesting to note that, although NFRC 102 requires that the emittance is to be used in the above equation, it does not specify anywhere whether to measure this value or use look-up tables. For the purposes of this project, the test facility followed its standard protocol, which is to use a typical value of 0.84, but the procedure should be specified more clearly in the Standard.

We recommend that the NFRC 102 Standard should clarify whether the emittance of the specimen is to be measured procedure, or if standardized values are to be used.

Specific Standards Language: NFRC 101 provides a method for measuring surface emittance, and also provides default values for many types of surfaces. Clause 6.5.2.2(A).a of NFRC 102 specifies that the tape used to hold thermocouples in place should be similar to the specimen, but as the emittance of the specimen is not known at this point, the requirement to measure the emittance (or use a default value) should be specified before this Clause. Our preference would be to use the default values in Appendix A of NFRC 101, to ensure a more standardized approach, but measured values should always be permitted in lieu of the default values.

The first term in equation <3> is convective, the second part is radiative, and so the components of the film coefficient as determined from testing can also be isolated. Thus, total and component parts of room-side film coefficients from test and simulation can be compared.

Table 3 Film coefficients for Specimen #1

	Test result	Simulation (galvanized)		Simulation (painted)	
		Result	% diff from test	Result	% diff from test
Surface temperature T_{is} , °C (°F)	-2.65 (27.2)	-12.6 (9.3)	N/A	-10.0 (14.0)	N/A
U-factor, $W/m^2 \text{ } ^\circ C$ (BTU/hr-ft ² -°F)	5.43 (0.96)	3.78 (0.67)	-43.7%	6.72 (1.18)	+19.2%
Weather-side film coefficient h_o , $W/m^2 \text{ } ^\circ C$ (BTU/hr-ft ² -°F)	30.0 (5.28)	25.77 (4.54)	-16.4%	30.93 (5.45)	+3.1%
Room-side film coefficient h_i , $W/m^2 \text{ } ^\circ C$ (BTU/hr-ft ² -°F) - total	6.75 (1.19)	4.13 (0.73)	-63.4%	7.97 (1.40)	+15.3%
- convective component	2.44 (0.43)	3.29 (0.58)	+25.8%	3.29 (0.58)	+25.8%
- radiative component	4.31 (0.76)	0.84 (0.15)	-413%	4.68 (0.82)	+7.9%

Although the documentation provided with THERM provides no description of the models used, it is assumed that the software follows the methods described in ISO 15099 (ISO, 2002). In this Standard, the convective portion of the room-side film coefficient is calculated from a correlation based on the Rayleigh number (which in turn depends on surface temperature, air temperature and the height of the specimen). The radiative component of the film coefficient is determined using a modified radiosity model, with view factors calculated using Hottel's crossed-string method. The Hottel method provides

a two-dimensional approximation of the view factors between three-dimensional surfaces that exchange heat via radiation, and introduces a small error for the sake of increasing computational speed. The three-dimensional nature of the large specimens considered in this project is only important at the perimeter of the specimens, where some of the surfaces of the specimen exchange heat via radiation with other surfaces in the specimen. As this is a relatively small proportion of the overall specimen area, the error introduced by the Hottel approximation should be relatively small.

As noted, the THERM program assigns a fixed value to the convective portion of the film coefficient, depending on the frame type selected. For this case, the value is $3.29 \text{ W/m}^2 \text{ }^\circ\text{C}$ ($0.58 \text{ BTU/hr-ft}^2\text{-}^\circ\text{F}$), based on an assumed specimen height of 1 meter (3.3 feet) and an assumed mean surface temperature typical of a given frame type.

Although the simulation and test methods provide two different approaches to determine the film coefficient, they should produce similar results. Table 3 indicates that they do not, however, and it would be useful to determine why this is so. As we do not have a clear explanation of how THERM assigns its values, we have used equation <3> to investigate the effect of the base assumptions on the results. We do this by adjusting each of the variables in the test procedure until they exactly match the conditions in the simulation, to see whether agreement is obtained.

The base-case test conditions ($T_{ia} = 21.29^\circ\text{C}$, or 70.3°F ; $T_{is} = -2.65^\circ\text{C}$ or 27.2°F ; $H = 3048 \text{ mm}$ or $120''$; and $\epsilon = 0.84$) were varied, one parameter at a time, to examine the resulting changes in the total room-side film coefficient and its components. The results are listed in Table 4.

Table 4 Adjustment of film coefficients for Specimen #1

	Total film coefficient h_{STh}		Convective component		Radiative component	
	$\text{W/m}^2\text{ }^\circ\text{C}$ ($\text{BTU/hr-ft}^2\text{-}^\circ\text{F}$)	% diff from simulation	$\text{W/m}^2\text{ }^\circ\text{C}$ ($\text{BTU/hr-ft}^2\text{-}^\circ\text{F}$)	% diff from simulation	$\text{W/m}^2\text{ }^\circ\text{C}$ ($\text{BTU/hr-ft}^2\text{-}^\circ\text{F}$)	% diff from simulation
Base Case	6.75 (1.19)	-8.5%	2.44 (0.43)	-25.8%	4.31 (0.76)	+5.4%
Air temperature = 21°C (simulation standard)	6.73 (1.19)	-8.8%	2.44 (0.43)	-25.8%	4.29 (0.76)	+4.9%
Emittance = 0.90 (default value)	7.04 (1.20)	-4.6%	2.44 (0.43)	-25.8%	4.60 (0.81)	+12.5%
Specimen height = 1 m (simulation assumption)	7.82 (1.38)	+6.0%	3.22 (0.57)	-2.1%	4.60 (0.81)	+12.5%
$T_{is} = -10^\circ\text{C}$ (to match simulation result)	7.88 (1.39)	+6.8%	3.45 (0.61)	+4.9%	4.43 (0.78)	+8.3%
$\epsilon = 0.20$ (to match galvanized simulation)	4.43 (0.78)	+7.3%	3.45 (0.61)	+4.9%	0.98 (0.17)	+16.7%

As Table 4 shows, the total film coefficient from testing can vary from -8.5% to +7.3%, relative to the simulation result, depending on the values chosen for the variables. There could be a combination of values for these variables that would provide an exact match between test and simulation, but that would be begging the question. Even the closest agreement between test and simulation in Table 4 is somewhat misleading, as it is the result of errors in the components (-25.8% on the convective portion and +12.5% on the radiative portion) canceling each other to produce a net difference of -4.6%.

The largest difference in successive changes to the total film coefficient occurred when the specimen height was changed from 3048 mm or 120" (the actual specimen height) to 1 m or 39.4" (the assumed height in THERM). This suggests that the one-meter assumption in THERM is a significant source of the differences between the test and simulation results for these products. This might not be apparent for typical residential products, which are closer to the assumed 1 m (39.4") in height, and for which the controlling thermal resistance is not the room-side film coefficient. For typical residential specimens, the error introduced by the one-meter assumption may not be significant, but it appears to be a problem for large, high-conductance products such as Specimen #1. It would be useful if THERM were modified to allow users to input the actual specimen height.

Changing the surface emittance from 0.84 (the value used in the test) to 0.90 (the default value in NFRC 101 Appendix A) made a difference of approximately 4% in the total film coefficient, relative to the simulation. The relative change in the radiative component of the film coefficient was rather large, as the difference between the test and simulation results went from +4.9% to +12.5%, but the difference in the total-product U-factor would be less than 4%. The difference between $\epsilon = 0.90$ (painted surface) and $\epsilon = 0.20$ (galvanized surface) is quite significant, as noted previously, and the difference between the radiative component of the film coefficient as predicted by equation <3> and the value predicted by simulation doubled from +8.3% to +16.7%.

Changing the room-side surface temperature T_{is} from the value measured in the test (-2.65°C or 27.2°F) to the value predicted by simulation (-10°C or 14°F) produced a significant increase in the difference between the test and simulation results for the convective portion of the film coefficient, and a slightly smaller decrease in the radiative component. The net result was a slight increase in the difference between test and simulation results for the total film coefficient.

In summary, the test and simulation methods use two different approaches to determine film coefficients. The derivation used in the test method is based on an empirical correlation, whereas the simulation method uses a model based on fundamental heat-transfer principles, but with some simplifying assumptions. In the case of a non-insulated specimen (e.g., Specimen #1), where the controlling resistance is the room-side film coefficient, the two different approaches produce results that are too dissimilar to provide a sufficient level of comfort to rely on the computer simulation as being representative of the test.

The simulation and test methods used in this project do not appear to provide an accurate representation of thermal performance for the non-insulated sectional garage door. We do not recommend using computer simulation to expand the scope of products represented in the design tables of the Handbook of Fundamentals for non-insulated doors in this project.

We recommend that the THERM program should be modified to allow users to input actual specimen height.

We recommend further study of the methods used to determine film coefficients in test and computer-simulation procedures, to develop a method that provides consistent results. Alternatively, equation <3> (from Clause 8.2.9.1 in NFRC 102) could be programmed into the software, which would then solve for T_{is} and adjust h_{STh} accordingly to achieve an iterative solution.

4.2 INSULATED SECTIONAL GARAGE DOOR

Specimen #2 was a steel sectional garage door manufactured by Garaga Industries Ltd. (see Figure 12). The door sections were nominally 44.5 mm (1¾") overall thickness, constructed of 26-gauge hot-galvanized steel sheets on either side of a pressure-injected polyurethane-foam core. The steel skins were painted white, and separated with a thermal break (see Figure 13). The ends of the door panels were closed with painted wooden stile blocks provide continuity of the thermal break.

Joints between sections were rabbeted to form a weather seal (but not an air seal), which is also visible in Figure 13. Any accessories to the door (e.g., hinges, handles and electric opener) are attached through the door skin to 14-gauge reinforcement plates on the interior of the door.

Galvanized hardware provided with the door included graduated end-roller hinges, intermediate hinges, adjustable top roller brackets, steel operator cable (see Figure 13), and galvanized steel tracks on either side, to represent typical installation.

The steel door tracks normally extend onto the ceiling of a garage, to guide the door sections as the assembly opens. The door tracks in the test specimen were cut to prevent interference with the constant-temperature baffle and air circulation during the thermal testing (see Figure 11).

The bottom of the door included a weather seal made of a U-shaped extruded vinyl bulb seal, typical this type of installation.

As was the case with Specimen #1, perimeter seals the jambs and head of the door assembly are optional accessories, but are often not installed as they may interfere with door operation. The perimeter seals were not installed in this specimen the air-leakage testing (and are not applicable to the thermal testing, as the product was sealed for the thermal test, as required in ASTM C1199).

The specimen is shown in Figure 12 installed in the mask wall, and was moved with the mask wall from the air-leakage test chamber to the thermal test chamber as a unit.



Figure 12 Specimen #2 Insulated Sectional Garage Door (in mask wall)



Figure 13 Edge view of Specimen #2 shows thermal break and weather seal (exterior is on the left in this figure)

4.2.1 Air-leakage testing

The insulated garage door was tested for air leakage following NFRC 400 procedures. The air-leakage test results for the non-insulated sectional door are shown in Appendix B. The results show good agreement with the classic formulation of air-leakage models, $Q = C \delta P^{0.65}$. For this specimen, air leakage varies with applied air pressure according to:

$Q = 0.05 \delta P^{0.65}$, where Q is air leakage in L/s per m^2 and δP is air-pressure difference in Pa (or $Q = 0.357 \delta P^{0.65}$, if Q is measured in cfm per ft^2 and δP is measured in inches of water).

At 75 Pa pressure difference (the standard criterion for NFRC 400), the air leakage for this product was measured to be 0.85 L/s per m^2 of projected area (0.17 cfm per ft^2). This actually meets the code-based requirement for swinging doors, which specifies a maximum air leakage of 1.88 L/s per m^2 (0.37 cfm per ft^2), but it is the only specimen in this study that achieved that level of airtightness. This is perhaps the only specimen in the study for which the most important purpose of the assembly is energy efficiency, as this product is intended to provide a reasonable amount of thermal resistance to a semi-conditioned space (i.e., the garage) in a cold climate.

4.2.2 U-factor testing

The insulated sectional door was tested in accordance with NFRC 102. The product tested was 2.74 m x 2.13 m (9' x 7'), which is the rough opening size. The test product is slightly larger, due to the door frame (see Figure 10), but the frame would not be included in the overall U-factor calculation in a load calculation, and therefore was not included in these test results. This size was chosen because it is the most common size for this product type – although the test size is slightly different from that specified in NFRC 102, which is 3 m x 2.39 m (118" x 94").

The results of U-factor testing for this product are shown in Appendix B, which also includes photographic representation of the products with thermocouple readings superimposed on the images to indicate the as-tested temperature distribution on both side of the specimen. The as-tested transmittance for the initial test of Specimen #2 is shown in Table 5.

Table 5 Specimen #2 Initial Test Results

As-tested	Area-weighting method					CTS method				
	U_s	T_{is}	h_i	T_{os}	h_o	U_{stA}	T_{is}	h_i	T_{os}	h_o
2.00 (0.35)	15.03 (59.1)	13.35 (2.35)	-16.19 (2.9)	47.38 (8.34)	1.72 (0.96)	12.6 (54.7)	9.40 (1.66)	-15.0 (5.1)	27.05 (4.76)	1.85 (0.33)

Note: Temperatures t_i and t_o in $^{\circ}C$ ($^{\circ}F$), U-factors and film coefficients h_i and h_o in $W/m^2 \cdot K$ ($BTU/hr \cdot ft^2 \cdot ^{\circ}F$)

For this specimen, the main contribution to the thermal resistance of this product is not the room-side film coefficient, as was the case with Specimen #1. The prediction of surface temperatures and film coefficients is similar for the two methods of standardizing the results, so the standardized thermal transmittances (U_{stA} and U_{stB}) are not that different. Both the ASTM C1199 and NFRC 102 procedures suggest that the CTS method is preferred for this type of product..

The measured surface temperatures for this product (see Appendix B) indicate a relatively constant condition at the warm surface, except that the top of the door was approximately 5.5 $^{\circ}C$ (10 $^{\circ}F$) colder than the adjacent surfaces. No reason for this difference was immediately apparent (see discussion in the next section).

4.2.3 U-factor Simulation

The simulation models used to represent this product, and the resulting component and area-weighted U-factors, are shown in Appendix B. The first simulation produced a total-product U-factor of 1.29 W/m²-K (0.23 BTU/hr-ft²-°F), well below the tested values (U_s or U_{st}), which indicated that the simulation model was not accounting for all of the heat transfer in the test specimen. The more conventional area-weighting method for determining U-factors (used to evaluate windows) was employed, and increasing the amount of edge-of-panel region in the models was also investigated (as was done in the case of Specimen #1 – see Section 4.1.3).

These corrections did not account for the differences between test and simulation, however, so other reasons for differences were explored. Thermal bridges created by bolts, reinforcing elements and other highly conductive components were specifically included in the models, but these adjustments did not make a significant difference in the overall result. This indicates that thermal bridging is not a serious concern for this product, but a significant problem still existed in the context of achieving a validated simulation model. The final simulation result for this specimen, accounting for increased edge effect, was a thermal transmittance of 1.59 W/m²-K (0.28 BTU/hr-ft²-°F).

The project team returned to the anomalous temperature reading from the test result (see Section 4.2.2). Several reasons for this unusual result were postulated, one of which was the possibility that the door had been manufactured with voids in the insulated core. The door was taken apart (see Figure 14) and the insulated core was examined. No voids or significant thermal bridges were observed.

The project team decided to re-test the specimen, hypothesizing that such a large insulated product might deflect under a 39°C (70°F) temperature difference. A new panel was obtained from the manufacturer, and the specimen was re-installed in the test chamber. During re-test, it was observed that the specimen did deflect. This did not occur in Specimen #1, as that door assembly was essentially isothermal.

The air seal for Specimen #2 was examined and found to have separated from the mask wall. It then became apparent that the test results were being contaminated with air leakage. The test chamber was opened, and a new air seal was installed in a way that would allow for deflection of the specimen without breaking the air seal. The specimen was re-tested, with the new results shown in Table 6.



the
to

Figure 14 Specimen #2 Disassembled

Table 6 Specimen #2 Final Test Results

As-tested	Area-weighting method					CTS method				
U_s	T_{is}	h_i	T_{os}	h_o	U_{stA}	T_{is}	h_i	T_{os}	h_o	U_{stB}
1.60 (0.28)	-2.65 (27.2)	10.21 (1.16)	-3.65 (25.4)	17.28 (5.28)	1.45 (0.26)	-3.75 (25.2)	9.72 (1.71)	-8.80 (16.2)	27.05 (4.76)	1.51 (0.27)

Note: Temperatures t_i and t_o in °C (°F), U-factors and film coefficients h_i and h_o in W/m²-K (BTU/hr-ft²-°F)

This result provides agreement between test and simulation of 8.8% (for the area-weighted method) and 5% (for the CTS method).

Section 8.2 of ASTM C1199 recommends that the CTS method should be used for this product. Using either approach meets the validation criterion of the NFRC 100 procedure, however, so the simulation model appears to provide a reasonably accurate representation of the thermal performance of Specimen #2 as well.

The key finding from the evaluation of this specimen arises from the results observed during the re-test. The difference between the two test results ($2.00 \text{ W/m}^2\text{-K}$ or $0.35 \text{ BTU/hr-ft}^2\text{-}^\circ\text{F}$ and $1.60 \text{ W/m}^2\text{-K}$ or $0.28 \text{ BTU/hr-ft}^2\text{-}^\circ\text{F}$) is due to the effect of air leakage. This means that, even though the test chamber was pressure-equalized across the specimen, the difference of 20% between a sealed thermal test and an unsealed test is quite significant. Thus, earlier test procedures that allowed an unsealed but pressure-balanced test may have produced test results that included the partial effects of air leakage.

It appears that a pressure-balanced test protocol is not sufficient to eliminate the effects of air leakage in a thermal test. We therefore recommend that test procedures for thermal transmittance should always require sealing against air leakage.

Specific Standards Language: the above recommendation is in keeping with NFRC procedures.

Further, a large test specimen with a reasonably low thermal transmittance may exhibit significant deflection when subjected to a large temperature difference. We therefore recommend that such products should be sealed against air leakage in such a manner that anticipates some movement as a result of this deflection, and maintains the air seal for the duration of the test. This deflection should also be kept in mind when calculating the heating, cooling and ventilation loads for a building during the design stage.

Specific Standards Language: Clause 5.1.5(A) of NFRC 102 could be modified by adding the sentence: "For large specimens (i.e., above 2m x 2m), the seal should be constructed so as to anticipate movement of the specimen due to thermal stresses."

We also recommend including a larger portion of edge-of-panel in the 2D model for this type of product (similar to the recommendation for Specimen #1).

Specific Standards Language: as per Section 4.1.3 of this report.

The modified simulation and test methods used in this project appear to provide an accurate representation of thermal performance for the insulated sectional garage door. We recommend using computer simulation to expand the scope of products represented in the design tables of the Handbook of Fundamentals for this project.

4.3 THREE-WING REVOLVING DOOR

Specimen #3 was a three-wing glazed revolving door, manufactured by the Boon Edam Corporation (see Figure 15). The door comprises three panels, two curved sidewalls and a canopy manufactured from aluminum extrusions. The standard sidewall construction utilizes a vertical end post on each side and one post in the center (where the door assembly connects to the exterior wall of a building, or in this case to the mask wall of the test chamber). The door panels are attached to the center shaft with two hangers on each wing, which allow the panels to be held in position with a preset tension and to be folded outward to allow for emergency egress.

The hardware that allows the door panels to collapse during an emergency exit is housed in floor below the central shaft. This hardware cannot be removed from the specimen, as the integrity of the door panels rests on it. This necessitates that the specimen must be elevated approximately 500 mm (20"). Therefore, the mask wall included a "mask floor", constructed of expanded polystyrene foam insulation. Due to depth of this specimen, a special thermal chamber was constructed (see Figure 15).

The door panels and curved sidewalls of the specimen were glazed with 6 mm (1/4") clear tempered safety glass.

The specimen was shipped unassembled, and manufacturer visited the facility to ensure that product was assembled correctly, as would be the case for a commercial product shipped to a construction site.



Figure 15 Specimen #3 in the test chamber

The joints between the operable door panels and the outer barrel of the assembly are weatherstripped to reduce air and water leakage. Weatherstripping options include felt and horsehair. The latter, which is standard on this particular product, has been used historically as a weatherstripping material because it is hydrophilic (i.e., expands as it absorbs moisture), so that the weather seal becomes tighter as the horsehair gets wet.

The specimen was tested at a nominal size of 3.05 m x 3.05 m (10' x 10'), which is the actual size of the mask-wall opening.

4.3.1 Air-leakage testing

The specimen was tested with both weatherstripping options (i.e., horsehair and felt), in two configurations (Figure 16). The "Delta" configuration is typical of the door's locked position at nighttime, but the "Wye" position is more typical during daytime operation.

Thus, four sets of air-leakage tests were conducted on this specimen, each at three different air-pressure differences.

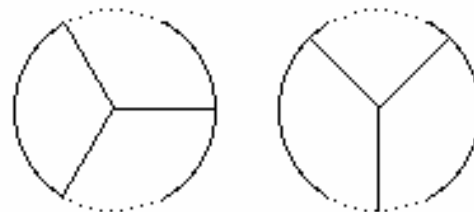


Figure 16 Plan view of a 3-wing door, showing "Delta" (left) and "Wye" (right) configurations

The air-leakage test results for the three-wing revolving door are shown in Appendix C, and summarized in Table 7. The results for horsehair show good agreement with the classic formulation of air-leakage models, $Q = C \delta P^{0.65}$, but felt weatherstripping appeared to provide better resistance to air leakage as tested, and it would be more appropriate to use $Q = C \delta P^{0.565}$ for this assembly. Note that the specimen was not tested in a wet environment, in which case we would expect the results for horsehair weatherstripping to improve, and the results for felt to get slightly worse.

Table 7 Summary of Air-leakage Test Results for the Three-wing Revolving Door

Configuration	Air leakage @ 75 Pa, L/s per m ² (@ 0.3 inches H ₂ O, cfm/ft ²)	Correlation, Q in L/s per m ² (or cfm per ft ²), δP in Pa (in. H ₂ O)
Horsehair, delta configuration	51.5 (10.1)	$Q = 3.04 \delta P^{0.65}$ (= 21.66 $\delta P^{0.65}$)
Horsehair, wye configuration	83.9 (16.5)	$Q = 5.04 \delta P^{0.65}$ (= 35.88 $\delta P^{0.65}$)
Felt strip, delta configuration	28.9 (5.6)	$Q = 2.38 \delta P^{0.565}$ (= 10.62 $\delta P^{0.565}$)
Felt strip, wye configuration	36.2 (7.1)	$Q = 3.03 \delta P^{0.565}$ (= 13.53 $\delta P^{0.565}$)

The specimen in the “delta” configuration produces lower air-leakage measurements than in the “wye” configuration (see Figure 16). This is not unusual, as the former provides three points of contact for the weatherstripping between the door panel and the barrel of the door, and the latter has only two contact points. As we have suggested that the “wye” configuration is more typical of daytime operation, however, the air-leakage results might be more appropriate for design considerations, unless the door assembly has an automatic closure device that returns the door to the “delta” configuration when not in use.

This specimen is the most leaky of all those tested in this study, even when tested in the “closed” (i.e., “delta”) configuration. This product is less concerned with energy efficiency as it is with ease of entrance and egress, so these results are perhaps not too surprising, although the “wye” results should be compared with an *open* swinging door, which would prove to be much leakier.

4.3.2 U-factor testing

As noted in Section 4.3, this specimen included a mask floor (see Figure 15) to isolate some of the operating hardware during the thermal test. This entrance system is installed in all types of flooring, so it was important to exclude the effect of the flooring system from the evaluation of this product.

The calibration exercise for this product, following the CTS method described in NFRC 102, was as follows: a standard planar CTS was built to fit into the rough opening in the mask wall of the test chamber. Air was directed vertically up the exterior surface of the mask wall containing the CTS, and the exterior wind speed necessary to develop a weather-side surface heat transfer coefficient of 26 - 29 W/m²-K (4.6 - 5.1 BTU/hr-ft²-°F) was measured. When the CTS was replaced with the revolving-door specimen, the same exterior air velocity was maintained around the curved exterior surface of the specimen, so that the convective film coefficient would be similar in both cases. This was a departure from the scope of the project, as a standard ASTM C1199 test would not include the CTS method (the ratio of the projected area to total surface area of the specimen is less than 0.8, so ASTM specifies that the area-weighted method should be used to standardize the test results. The project team wished to determine which method of standardizing the results was appropriate for this specimen, by comparison with simulation.

The results of U-factor testing for this product are shown in Appendix C, and summarized in Table 8. The as-tested U-factor was $U_s = 5.75 \text{ W/m}^2\text{-K}$ ($1.01 \text{ BTU/hr-ft}^2\text{-}^\circ\text{F}$). When corrected using the area-weighting method the resulting standardized transmittance was $U_{st} = 4.66 \text{ W/m}^2\text{-K}$ ($0.82 \text{ BTU/hr-ft}^2\text{-}^\circ\text{F}$) and the CTS method produced $U_{st} = 3.67 \text{ W/m}^2\text{-K}$ ($0.27 \text{ BTU/hr-ft}^2\text{-}^\circ\text{F}$).

The standardized result using the CTS method shows a large variance between the as-tested and standardized values, and a significant difference between the area-weighting method and the CTS method. As noted, the ASTM C1199 procedure would require that the area-weighted results should be used, because the specimen projects so far out of the plane of the mask wall. This is evident from the large difference in film coefficients shown in Table 8.

Table 8 Specimen #3 Test Results

As-tested	Area-weighting method					CTS method				
U_s	T_{is}	h_i	T_{os}	h_o	U_{stA}	T_{is}	h_i	T_{os}	h_o	U_{stB}
5.75 (1.01)	5.94 (42.7)	15.01 (2.64)	-15.0 (5.0)	69.31 (12.2)	4.66 (0.82)	10.3 (50.5)	21.11 (3.72)	-9.93 (14.1)	27.05 (4.76)	3.67 (0.65)

Note: Temperatures t_i and t_o in $^\circ\text{C}$ ($^\circ\text{F}$), U-factors and film coefficients h_i and h_o in $\text{W/m}^2\text{-K}$ ($\text{BTU/hr-ft}^2\text{-}^\circ\text{F}$)

We recommend that ASTM C1199 should be followed regarding area-weighting vs. CTS methods for the revolving-door specimens (because $A_p \ll A_s$).

4.3.3 U-factor Simulation

As noted in Section 3.4, the unusual configuration of this door type introduces more complexity to the simulation procedure. Apart from the natural convection inside the pie-shaped chamber formed by the closed door (see Figure 16), convective and radiative heat transfer on the weather-side and room-side of the specimen will be unusual. The interesting geometry formed by the intersection of the door cylinder with the wall in which it is mounted, and by the centre V formed by the closed door panels, will produce complex airflow patterns on the exterior surface. This is not apparent in the U-factor, however, because the calculation of film coefficients in ASTM C1199 assumes that they are applied uniformly over the (room-side and weather-side) surfaces of the specimen. The same uniform application of film coefficient occurs in the simulation procedure, so local variations in these conditions (which almost certainly occur in the test specimen) are not considered in the overall heat transfer evaluation. Thus, the procedure would not be appropriate for evaluating local surface temperatures for condensation potential.

The method for determining the U-factor of a revolving door using computer simulation follows the general underlying philosophy behind the original NFRC simulation procedures. As noted in Section 3.3 of this report, the basic concept of the calculated U-factor involves an area-weighted average of all component U-factors, where an individual component model (frame and “edge-glass” assembly) defines a unique cross-section of the total product. The difficult part is in determining which cross-sections should be used to characterize the component parts of the overall product.

In the case of a three-wing revolving door, for example, the left and right head sections would represent unique components of the overall assembly. Representative two-dimensional models of these sections would include a portion of the mask wall above the product, the canopy, and the upper part of the door panel (incorporating the edge-glass region of the door panel, at least 63.5 mm or 2.5” away from the sightline). Figures 17 and 18 show typical locations where representative sections would be taken through the specimen to develop the models.

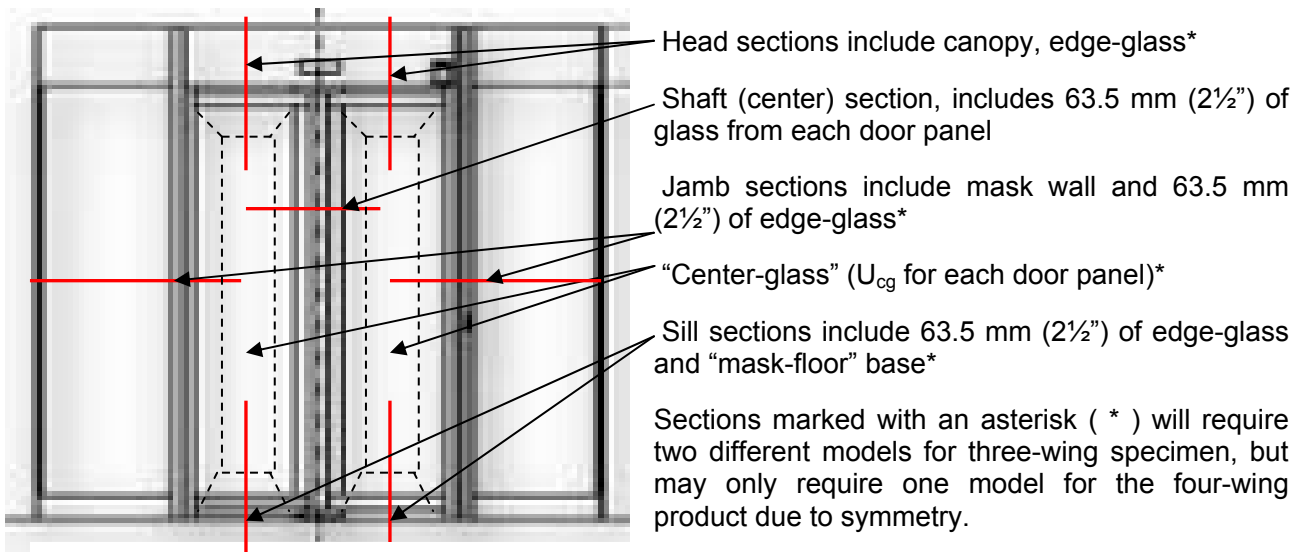


Figure 17 Elevation View of Revolving Door

The models for the single-panel portion of the three-wing door (at right in Figure 18) are relatively simple. The sections with the air cavity of the door chamber (at left in Figure 18) are more complicated, due to the convective flow in the enclosed cavity. As described in Section 3.4, a CFD model was used to calculate an effective thermal conductivity that accounts for increased heat flow due to convection within the enclosed cavity. The average effective thermal conductivity of the air cavity was used in the simplified 2D model to obtain average heat flow (and thus the component U-factor) for all appropriate cross-sections. These values were area-weighted to produce an overall U-factor for the assembly.

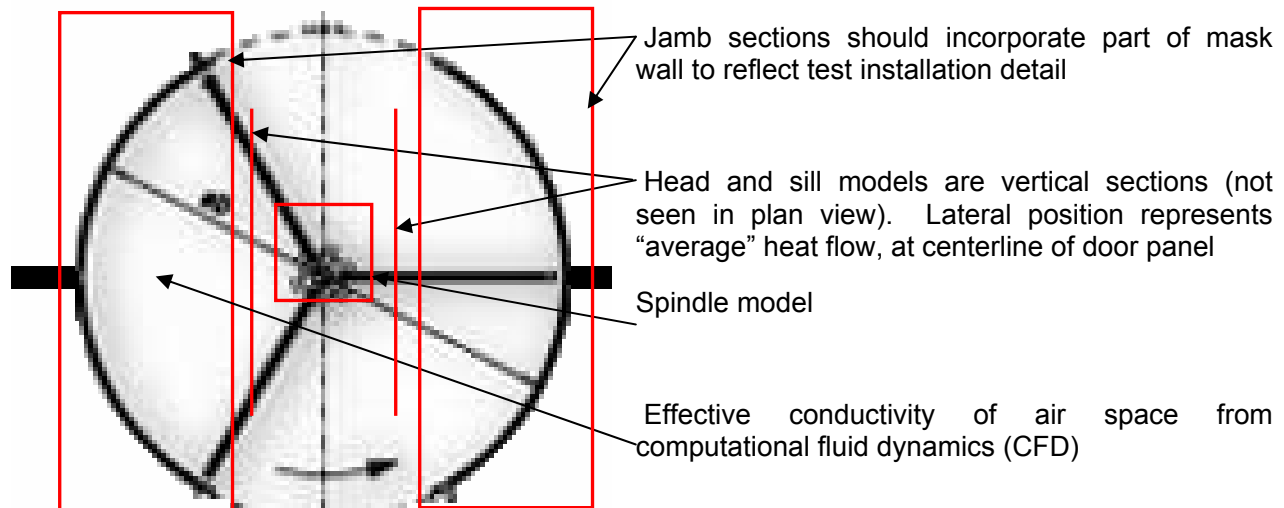


Figure 18 Horizontal Section of Specimen #3 (Three-wing Revolving Door)

The portion of the assembly not included in the 2D models is the analog of center-glass areas in a conventional planar window. This is the area that can be approximated by one-dimensional heat flow that occurs near the center of the door panel: this would be accurate for the single-panel section (again, the right-hand portion of Figure 18), but only an estimate of the heat flow through the center of

the enclosed air cavity. The overall heat transfer would theoretically be reasonably accurate on average for that product at that size, but could not be extrapolated to other cases. Assuming that this approach provided good agreement with the test results, however, we would be able to generate representative values for the effective thermal conductivity of enclosed air cavities using CFD runs for other configurations (see Section 3.4).

The 2D models used to generate total-product U-factors for the three-wing door are shown in Appendix C, together with the resulting component and area-weighted U-factors. The simulation produced a total-product U-factor of 4.53 W/m²-K (0.80 BTU/hr-ft²-°F), which is 2.9% lower than the test result using the area-weighted method, and 19% higher than the test result for the CTS method. As stated previously, the ASTM procedure specifies the area-weighting method. Thus, this approach appears to provide a very accurate representation of the thermal performance of the three-wing revolving door. It would appear that this simulation approach is appropriate for this type of product.

The simulation method used in this project appears to provide an accurate representation of thermal performance for the three-wing revolving door. The area-weighting method of standardizing test results also appears to provide good agreement with simulation for this case. As this procedure is experimental, however, we do not recommend its use in expanding the scope of results for this project until more validation can be done on these types of products in subsequent research.

4.4 FOUR-WING REVOLVING DOOR

Specimen #4 was a four-wing glazed revolving door, manufactured by C J Rush Industries Ltd. (Figure 19). The door comprised four panels, two curved sidewalls and a canopy manufactured from extruded aluminum. The curved sidewalls have a vertical end post on each side and one in the center (where the door connects to the exterior wall of a building, or in this case to the mask wall of the test chamber). The door panel construction is similar to that of the three-wing specimen, and also features a pressure-release mechanism below floor level to allow the door panels to collapse during emergency exit. Therefore, the specimen was built on a “mask floor” of expanded polystyrene foam below the mask wall.



Figure 19 Specimen #4 in Test Chamber

Door panels and curved sidewalls of the specimen were glazed with 1/4” clear tempered safety glass. Weatherstripping provided was the manufacturer’s standard option, reinforced neoprene seals at the head and sills, with felt sweep seals reinforced with a neoprene fin at the door stiles.

The specimen was shipped unassembled, and the manufacturer visited the facility to ensure that the product was assembled correctly, as would be the case for a commercial product shipped to a construction site. The specimen was tested at a nominal size of 2.74 m x 2.13 m (9’ x 7’), which is the actual size of the mask-wall opening shown in Figure 19. This size is typical of a standard pedestrian entrance for a commercial building (e.g., bank or retail store).

4.4.1 Air-leakage testing

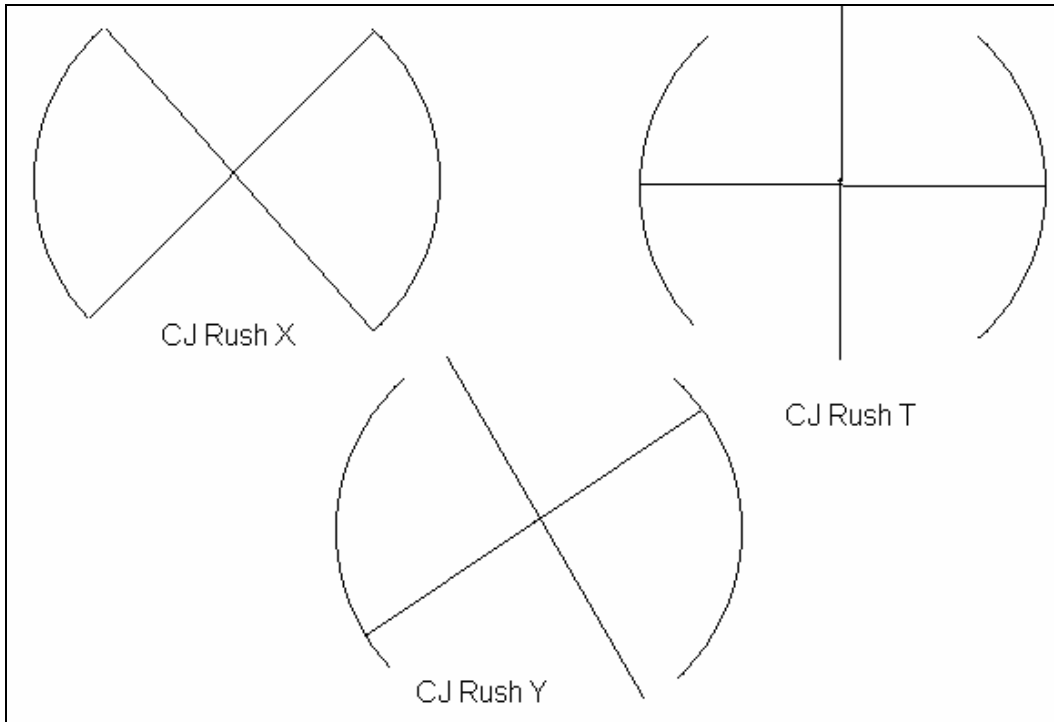
The specimen was tested in three different configurations, as shown in Figure 20. The “X” configuration is typical of the door’s locked position at nighttime, and the “T” and “Y” positions represent typical daytime operation. Thus, three air-leakage tests were conducted on this specimen, each at three different air-pressure differences. The air-leakage test results for the three-wing revolving door are shown in Appendix C, and summarized in Table 9.

All results for this specimen show good agreement with the classic formulation of air-leakage models, $Q = C \delta P^{0.65}$. The specimen in the closed (“X”) position is the most airtight, and the “Y” configuration is almost twice as leaky that the “T” configuration. An applied pressure difference in the “T” configuration moves the door assembly in a balanced way against the seals. The “Y” configuration, on the other hand, is asymmetrically positioned, so an applied pressure difference does not seal equally on both sides of the door assembly, resulting in higher air leakage.

Table 9 Summary of Air-leakage Test Results for the Four-wing Revolving Door

Configuration	Air leakage @ 75 Pa, L/s per m ² (@ 0.3 inches H ₂ O, cfm/ft ²)	Correlation, Q in L/s per m ² (or cfm per ft ²), δP in Pa (in. H ₂ O)
X (closed)	8.9 (1.75)	$Q = 0.55 \delta P^{0.65} (= 3.94 \delta P^{0.65})$
T	14.02 (2.76)	$Q = 0.86 \delta P^{0.65} (= 6.15 \delta P^{0.65})$
Y	26.3 (5.18)	$Q = 1.6 \delta P^{0.65} (= 11.45 \delta P^{0.65})$

Figure 20 Configurations for Specimen #4 Air Test



4.4.2 U-factor testing

The thermal tests were conducted with a mask wall in place of the exterior wall shown. The mask wall intersected the barrel of the door at its midplane, and the roof of the barrel was exposed to the warm-side and cold-side test chambers in the same way as the actual product is exposed to the room and weather when installed in its normal configuration (see Figure 7).

The U-factor test results for Specimen #4 are shown in Appendix D and are summarized in Table 10.

Again, ASTM C1199 specifies that the area-weighting method should be used for projecting products such as this specimen.



Figure 21 Specimen #4 in the test chamber

Table 10 Specimen #4 Test Results

As-tested	Area-weighting method					CTS method				
U_s	t_i	h_i	t_o	h_o	U_{stA}	t_i	h_i	t_o	h_o	U_{stB}
4.10 (0.72)	10.27 (50.5)	15.29 (2.69)	-16.0 (3.2)	72.65 (12.8)	3.48 (0.61)	12.7 (54.5)	19.95 (3.51)	-12.3 (9.9)	27.05 (4.76)	2.93 (0.52)

Note: Temperatures t_i and t_o in °C (°F), U-factors and film coefficients h_i and h_o in $W/m^2\cdot K$ (BTU/hr-ft²-°F)

4.4.3 U-factor Simulation

The method used to simulate the U-factor of the four-wing revolving door is similar to that described for the three-wing door (see Section 4.3.3). The procedure is simplified by exploiting the symmetry of the specimen, so that only four cross-sectional models are required (left or right head section, left or right jamb section, left or right sill section, and center shaft model: see Figure 22).

The 2D models used to generate total-product U-factors for the four-wing door are shown in Appendix D, together with the resulting component and area-weighted U-factors. The simulation produced a total-product U-factor of 3.63 $W/m^2\cdot K$ (0.64 BTU/hr-ft²-°F), which is 4.1% higher than the test result using area-weighting, and 19.3% higher than the CTS test result. As the area-weighting method is preferred, this simulation approach appears to provide a reasonably accurate representation of the thermal performance of the four-wing revolving door.

Four-wing

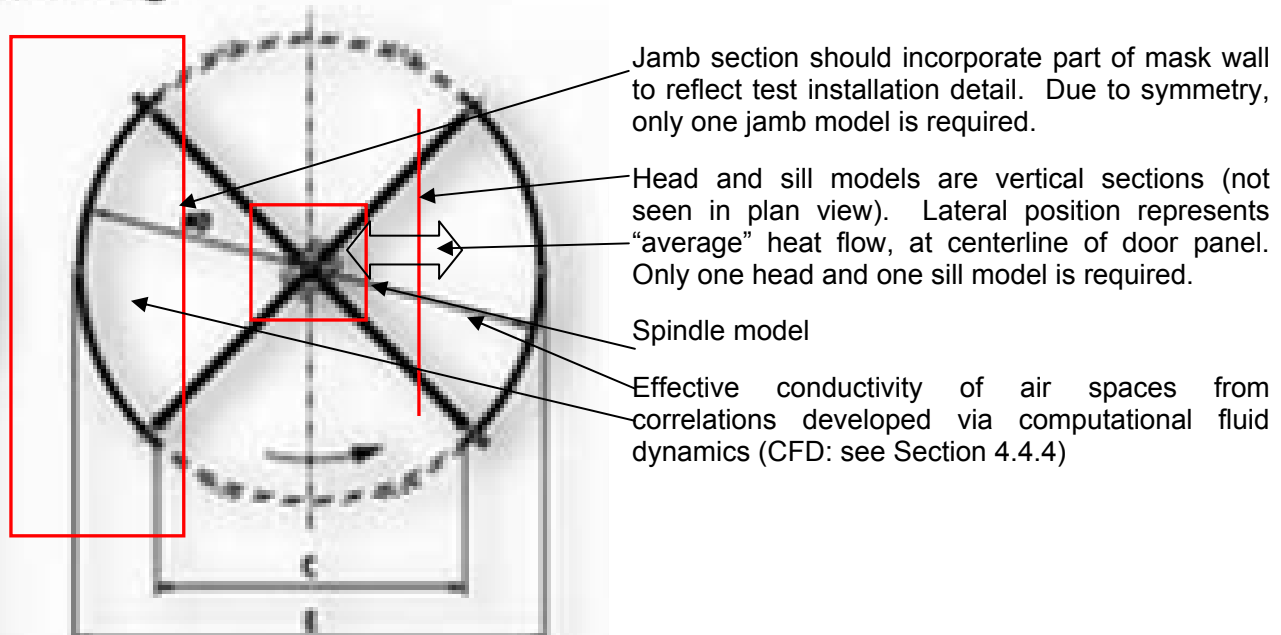


Figure 22 Horizontal Section of Specimen #4 (Four-wing Revolving Door)

The simulation method used in this project appears to provide an accurate representation of thermal performance for a 4-wing revolving door, but we do not recommend expanding the scope of results for this project without more validation on these types of products.

4.5 METAL COILING SLAT DOOR

Specimen #5 was a metal coiling slat door manufactured by the Overhead Door Corporation, similar to the product shown on the left-hand side of Figure 23. The product was mounted onto the room-side face of the mask wall with three metal angles (one at the head and one on each jamb), which is very typical in the industry. The opening in the mask wall was framed with wood plates (38 mm x 190 mm, or nominal 2" x 8").

The door comprises interlocking flat metal slats of 22-gauge galvanized steel. The product is also available with curved slats, which provide a more compact coil when the door is opened, but the curved slats do not work as well with weather seals when the door is closed.



Figure 23 Typical cargo bay, with metal coiling slat door (similar to Specimen #5) and a non-insulated sectional garage door (similar to Specimen #1)

The specimen was tested at a nominal size of 3.05 m x 3.05 m (10' x 10'), the actual size of the mask-wall opening. The specimen was installed in the mask wall by the manufacturer's local distributor, to ensure that the installation was typical of this product.

4.5.1 Air-leakage testing

Specimen #5 was tested for air leakage following NFRC 400 procedures. The air-leakage test results are shown in Appendix E. The results show good agreement with the classic formulation of air-leakage models, $Q = C \delta P^{0.65}$. Our analysis has determined that, for the specimen tested, air leakage varies with applied air pressure according to:

$Q = 1.34 \delta P^{0.65}$, where Q is air leakage in L/s per m^2 and δP is air-pressure difference in Pa (or $Q = 9.54 \delta P^{0.65}$, if Q is measured in cfm per ft^2 and δP is measured in inches of water).

At 75 Pa pressure difference (as per NFRC 400), the air leakage for this product was measured at 22.4 L/s per m^2 of projected area (4.41 cfm per ft^2). To provide context, air leakage for this specimen is approximately 12 greater than a code-based requirement for swinging doors, which specifies a maximum air leakage of 1.88 L/s per m^2 (0.37 cfm per ft^2). Again, as with most specimens in this study, the primary purpose of these assemblies is control of building access, and not necessarily airtightness or energy efficiency.

4.5.2 U-factor testing

Once the air-leakage testing for Specimen #5 was completed, the specimen (in the mask wall) was installed in the hot-box chamber for U-factor testing. The specimen was sealed on the exterior (i.e., the side closest to the primary seal, as specified in ASTM C1199). As Figure 24 shows, this required a significant amount of tape: the specimen had 42 seams between the slats facing the exterior, and the perimeter of the specimen required a great deal of sealing as well. The U-factor test results for Specimen #5 are shown in Appendix E and in Table 11.



Figure 24 Exterior View of Specimen #5 (sealed before U-factor test to prevent air leakage)

Table 11 Specimen #5 Test Results

As-tested	Area-weighting method					CTS method				
U_s	t_i	h_i	t_o	h_o	U_{stA}	t_i	h_i	t_o	h_o	U_{stB}
5.88 (1.04)	-1.67 (29.0)	10.03 (1.77)	-4.36 (24.2)	17.00 (2.99)	5.54 (0.98)	-1.99 (28.4)	9.90 (1.74)	-9.39 (15.1)	27.05 (4.76)	4.68 (0.82)

Note: Temperatures t_i and t_o in °C (°F), U-factors and film coefficients h_i and h_o in $W/m^2\cdot K$ (BTU/hr-ft²-°F)

Although this specimen is not a projecting product, ASTM C1199 requires that the area-weighting method should be used, as $U_s > 3.4 W/m^2\cdot K$ (0.60 BTU/hr-ft²-°F). Again, we see that this is appropriate, as Table 10 shows that the area-weighting method produces room-side and weather-side surface temperatures that differ by only 2.7 °C (4.8 F°), whereas the CTS method produces a temperature difference of 7.4 °C (13.3 F°). The CTS results imply a much larger thermal resistance than one would expect, given the geometry of the specimen.

Therefore, the recommendations regarding the use of the area-weighting method instead of the CTS method for high-conductance specimens, as mentioned in Section 4.1.3, hold true for this specimen as well.

4.5.3 U-factor Simulation

The simulation models used to represent this product, and the resulting component and area-weighted U-factors, are shown in Appendix E. The initial simulation produced a total-product U-factor of 7.86 W/m²-K (1.38 BTU/hr-ft²-°F), much higher than the tested values (U_s or U_{st}), which indicated that the simulation model was accounting for far too much heat transfer in the test specimen. The only significant contributor to thermal resistance for this product (and, therefore, the “controlling resistance” as defined in classical simulation theory) was the room-side film coefficient, as the product is essentially a metal sheet. Therefore, the characterization of the room-side film coefficient was suspected as the source of error for the simulation model.

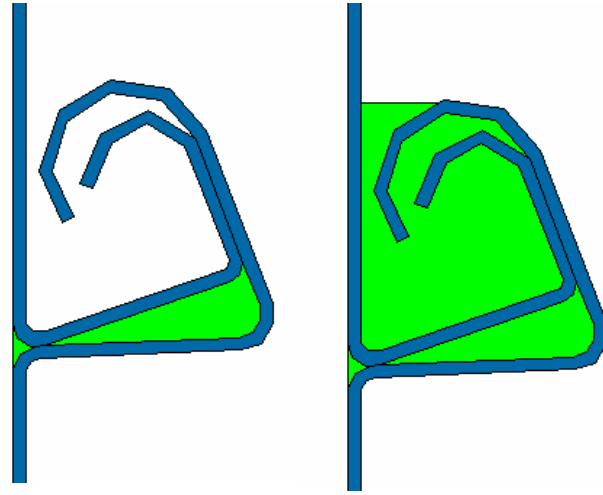


Figure 25 Cross-sectional Model showing fully wetted* surface (left) and enclosed air cavities (right) in the 2D simulation of Specimen #5

The application of the room-side film coefficient to the model is done automatically in the 2D program used to calculate the U-factor in NFRC100. If the room-side surface includes all of the intricate surfaces of the slats (seen on the left-hand side of Figure 25, the application of a film coefficient produces a huge wetted* surface area, which is not representative of the interaction between the specimen and the warm side of the test chamber.

Therefore, the model was modified to include a dead-air space inside the curled edge of the slats, as shown at right in Figure 25. This is expected to provide a more realistic approximation of the actual convective flow that would occur in the test configuration. There is no reason that the natural convective flow on the interior surface would follow into the partial cavity formed by the curled edges of the slats.

We recommend that the automatic use of a fully wetted* surface, as shown in Figure 25, should be reviewed to ensure that it does not produce unrealistic models in the case of complex articulated surfaces (e.g., metal coiling slat doors).

When this was applied to all cross-sections, the initial total-product U-factor from simulation was 5.88 W/m²-K (1.04 BTU/hr-ft²-°F). This is 5.8% higher than the area-weighted test result, and 20.4% higher than the CTS test result. The area-weighting method is preferred in ASTM C1199 (see Section 4.5.2), so simulation appeared to provide an accurate representation of the thermal performance of the roll-up door.

At this juncture in the research project, the discrepancy regarding Specimen #1 was discovered (see Section 4.1.3), and it was suspected that a similar problem may have occurred with Specimen #5. The testing laboratory verified that the surface of Specimen #5 was also coated with a primer, so the simulation results were recalculated using a painted surface. The resulting U-factor was 7.94 W/m²-K (1.40 BTU/hr-ft²-°F), which is well beyond the NFRC agreement criterion. The analysis of the results described in Section 4.1.3 was repeated for this specimen. This analysis is summarized in Table 12.

* In this context, “wetted” refers to a surface in thermal contact with the room air, to which the full effect of convective and radiative heat transfer is applied. In this case, a significant amount of surface area would not experience the convective flow characteristic of a full-height specimen, nor would those areas participate in radiative heat-transfer exchange with the surfaces in the room, and so should not be counted as part of the wetted area (i.e., should not have the full value of the film coefficient applied to those surfaces).

Table 12 Film coefficients for Specimen #5

	Test result	Simulation (galvanized)		Simulation (painted)	
		Result	% diff from test	Result	% diff from test
Surface temperature T_{is} , °C (°F)	-1.67 (29.0)	-11.7 (10.9)	N/A	-8.9 (16.0)	N/A
U-factor, $W/m^2 \text{ } ^\circ C$ (BTU/hr-ft ² -°F)	5.29 (0.93)	5.88 (1.04)	+10.0%	7.94 (1.40)	+33.4%
Weather-side film coefficient h_o , $W/m^2 \text{ } ^\circ C$ (BTU/hr-ft ² -°F)	30.0 (5.28)	25.48 (4.49)	-17.7%	34.0 (5.99)	+11.8%
Room-side film coefficient h_i , $W/m^2 \text{ } ^\circ C$ (BTU/hr-ft ² -°F) - total	6.74 (1.19)	6.46 (1.14)	-4.3%	8.79 (1.55)	+23.3%
- convective component	2.58 (0.45)	3.29 (0.58)	+21.6%	3.29 (0.58)	+21.6%
- radiative component	4.16 (0.73)	3.15 (0.55)	-32.1%	5.50 (0.97)	+24.4%

Table 12 shows that the good agreement between test and simulation for the galvanized specimen could be misleading. The total room-side film coefficient (and therefore the total-product U-factor, since the thermal resistance of this specimen is mainly due to h_i) shows good agreement, but this appears to result from the combination of a convective component that is much too large, and a radiative component that is much too small. When the change is made from a galvanized surface to a painted surface, the radiative component becomes large, and the differences in the components of the film coefficient no longer cancel each other out.

The effect of changing the variables (T_{ia} , T_{is} , H and ϵ) on the film coefficient were examined in Section 4.1.3 for Specimen #1, and it would be redundant to repeat the exercise here. What is not known – and what is impossible to evaluate within the scope of this project – is how THERM uses these variables in developing film coefficients in the computer models. Thus, the reasons for discrepancies between the NFRC test and simulation procedures for determining the film coefficients cannot be determined at this juncture. We can only repeat our recommendation that the reasons for these discrepancies should be investigated by someone with access to the source code for the computer model.

The simulation and test methods used in this project do not appear to provide an accurate representation of thermal performance for the non-insulated metal coiling slat door. We do not recommend using computer simulation to expand the scope of products represented in the design tables of the Handbook of Fundamentals for this project.

We recommend that the THERM program should be modified to allow users to input actual specimen height.

We recommend further study of methods used to determine film coefficients in test and computer-simulation procedures, to develop a method that provides consistent results. Equation <3> could be built into the software, which would then solve for T_{is} and adjust h_{STh} to achieve an iterative solution. The original approach allowed the user to specify a standardized film coefficient in the software, and this seemed to work reasonably well.

4.6 EMERGENCY EXIT DOOR

Specimen #6 was an emergency exit door, with honeycomb kraft-paper insulation sandwiched between two 18-gauge sheet-steel skins. The specimen is enclosed with 16-gauge steel channels on all sides, and reinforced with internal plates wherever hardware (e.g., panic bar, automatic door closure, hinges) are attached to the door. The product is manufactured by De La Fontaine Doors, and is typical of emergency-exit doors manufactured throughout North America. The product is available with a variety of optional insulating cores, but the honeycomb-paper option is more complex than other insulation types (which are homogeneous foamed insulation materials).

Therefore, it was considered that good agreement between test and simulation for this test specimen would provide a greater degree of confidence in the ability of the simulation model to produce accurate results for simpler insulation options. The specimen was tested at a nominal size of 1.02 m x 2.08 m (40" x 82"), the actual size of the mask-wall opening. This specimen was 44.5 mm (1 3/4") thick. The specimen was installed in the mask wall by the manufacturer's local distributor, to ensure that the installation was representative of this type of product.

4.6.1 Air-leakage testing

This product was tested for air leakage as per NFRC 400. The manufacturer offers many weatherstripping options. Some of these options were installed on the test specimen (see Figure 26), to provide a range of air-leakage characteristics for weatherstripping configurations representative of this type of product. This produced four different weather-seal configurations, tested at three different air pressures to produce a correlation curve (see Appendix F), for a total of 12 air-leakage tests for Specimen #6.

Air-leakage test results for Specimen #6 are shown in Appendix F. The results show good agreement with the classic formulation of air-leakage models, $Q = C \delta P^{0.65}$.

At 75 Pa pressure difference (the standard criterion for NFRC 400), the air leakage for this product was measured at a range of 3.95 – 10.6 L/s per m² of projected area (0.78 – 2.08 cfm per ft²), depending on the weatherstripping option. This specimen is therefore approximately twice as leaky as an equivalent swinging door, which may reflect the threshold for this product (accessibility is a requirement for emergency egress doors, so a zero-clearance threshold is standard).

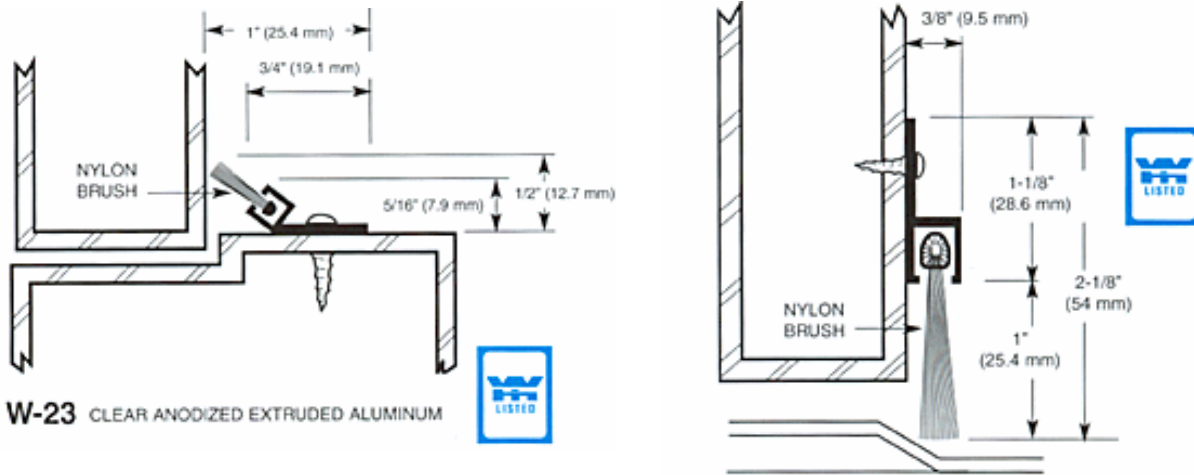
4.6.2 U-factor testing

The U-factor test results for Specimen #6 are shown in Appendix F, and show $U_s = 3.50 \text{ W/m}^2\text{-K}$ (0.62 BTU/hr-ft²-°F). Although this specimen is not a projecting product, ASTM C1199 requires that the area-weighting method should be used, as $U_s > 3.4 \text{ W/m}^2\text{-K}$ (0.60 BTU/hr-ft²-°F).

Table 13 Specimen #6 Test Results

As-tested	Area-weighting method					CTS method				
U_s	t_i	h_i	t_o	h_o	U_{stA}	t_i	h_i	t_o	h_o	U_{stB}
3.50 (0.62)	6.09 (43.0)	9.18 (1.62)	-14.71 (5.51)	38.67 (6.81)	3.11 (0.55)	8.65 (47.6)	11.07 (1.95)	-13.25 (8.15)	27.42 (4.83)	2.96 (0.52)

Figure 26 Various weatherstripping options tested for air leakage in Specimen #6

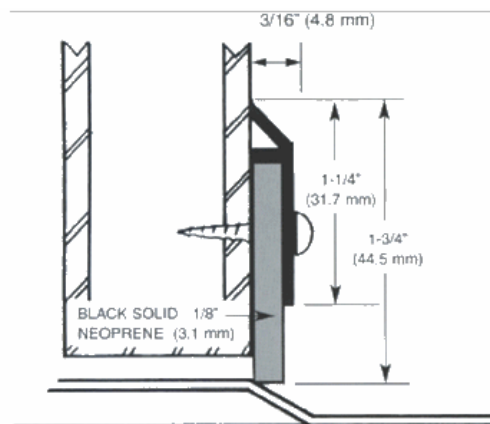
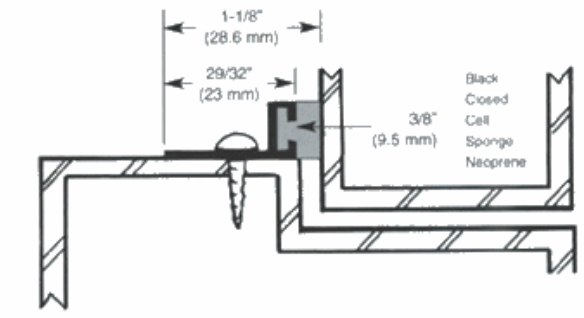


J140 head/jamb weatherstrip similar to this product

D-480 sill sweep similar to this product

W16N

Clear Anodized Extruded Aluminium



1650 head/jamb weatherstrip similar to this product

2100 door sill sweep similar to this product

4.6.3 U-factor Simulation

The method used to simulate the U-factor of the emergency exit door follows the conventional procedure outlined in NFRC 100, except that we again included a much larger edge-of-door region to ensure that all of the fin effect of the steel-skin door was captured. When following the conventional NFRC procedure (with no edge-panel region), the resulting total-product U-factor was of 2.64 W/m²-K (0.46 BTU/hr-ft²-°F), but including a 63.5-mm (2.5-inch) edge-of-slab region in the door model increased the total-product U-factor to 3.04 W/m²-K (0.53 BTU/hr-ft²-°F), which indicates that the conventional approach does not model part of the edge-of-panel loss. Increasing the edge dimension beyond 63.5 mm did not appreciably increase the U-factor, so it appears that this is adequate to achieve a representative result. This compares favorably with the test result, producing agreement of 2.6% between test and simulation.

The 2D models used to generate total-product U-factors for Specimen #6 are shown in Appendix F, together with the resulting component and area-weighted U-factors. This simulation approach appears to provide a reasonably accurate representation of the thermal performance of the insulated emergency exit door. As this door was insulated with honeycomb kraft-paper insulation, it is expected that simulation results for products with homogeneous foamed insulation will also be representative of test results.

We recommend including a larger portion of edge-of-panel in the 2D model for this type of product. It requires little additional effort to create the model, and greatly improves the accuracy of the result.

Specific Standards Language: where Figures 5-2a and 5-2b in NFRC 100-2004 indicates that the edge-of-panel area is 63.5 mm (2.5”), this should be changed to the 150 mm (6”) dimension developed in this study, but there is no guarantee that this would be suitable for all products.

The technically correct methodology, as was used in this project, is to incrementally increase the edge-of-panel height until subsequent iterations produce no change in the result, but this may not be desirable language in a Standard such as NFRC 100.

We recommend modifying Figures 5-2a and 5-2b in NFRC 100 so that the “edge-of-panel area” reads 150 mm (6”) instead of 63.5 mm (2.5”) – or so that it reads “Edge-of-Panel Area: height varies”, with a direction in the Simulation Manual to incrementally increase edge-of-panel height until subsequent iterations produce no change in the result.

The modified simulation and test methods used in this project appear to provide an accurate representation of thermal performance for the insulated emergency exit door. We recommend using computer simulation to expand the scope of products represented in the design tables of the Handbook of Fundamentals for this project.

4.7 AIRCRAFT HANGAR DOOR

Specimen #7 was an aircraft hangar door, custom-built for this project. The specimen was constructed of a 24-gauge HSS frame, comprising three panels. Each panel was built with a perimeter frame of 3/16” HSS and two intermediate horizontal mullions of 1/8” HSS. The exterior (weather-side) surface was clad with 26-gauge profiled steel, typical of the design of these systems, and the interior was finished with glass-fiber batt insulation and heavy-duty polyethylene. In a commercial application the interior finish would be an opaque (typically white) vinyl sheet product, but the project team wanted to be able to review the batts to ensure that no voids were present in the insulation (see Figure 27).

A single astragal (i.e., where the door panels from either side of the hangar would normally meet in the middle of the rough opening) and a single meeting stile were included in the specimen, to represent typically assembly of these components. The specimen included a steel frame mounted onto the mask wall, as would normally be included in a field installation. All normal operating hardware (rollers, hangers, etc.) were included in the assembly.

The specimen was tested at a nominal size of 3245 mm x 3245 mm (128” x 128”), the actual size of the mask-wall opening. The specimen was installed in the mask wall by the manufacturer’s local distributor, to ensure that the installation was typical of this product.



Figure 27 Specimen #7 installed in mask wall (viewed from interior and exterior)

4.7.1 Air-leakage testing

The aircraft hangar door was tested for air leakage following NFRC 400 procedures. The air-leakage test results for this specimen are shown in Appendix G. The results show good agreement with the classic formulation of air-leakage models, $Q = C \delta P^{0.65}$. For this specimen, air leakage varies with applied air pressure according to:

$Q = 0.54 \delta P^{0.651}$, where Q is air leakage in L/s per m^2 and δP is air-pressure difference in Pa (or $Q = 3.84 \delta P^{0.651}$, if Q is measured in cfm per ft^2 and δP is measured in inches of water).

At 75 Pa pressure difference (the standard criterion for NFRC 400), the air leakage for this product was measured to be 9.01 L/s per m^2 of projected area (1.77 cfm per ft^2).

This is approximately five times as leaky as the Code requirement for swinging doors (air leakage of 1.88 L/s per m^2 or 0.37 cfm per ft^2).

4.7.2 U-factor testing

The U-factor test results for Specimen #7 are shown in Appendix G, and show $U_s = 2.30 \text{ W/m}^2\text{-K}$ (0.41 BTU/hr- ft^2 -°F). The area-weighting method produced $U_{st} = 2.11 \text{ W/m}^2\text{-K}$ (0.37 BTU/hr- ft^2 -°F), and the CTS method produced $U_{st} = 1.92 \text{ W/m}^2\text{-K}$ (0.34 BTU/hr- ft^2 -°F). Although this specimen is not a projecting product, ASTM C1199 requires that the area-weighting method should be used, as the interior wetted area is much larger than the projected area. Test results for the aircraft hangar door are summarized in Table 14.

Table 14 Specimen #7 Test Results

As-tested	Area-weighting method					CTS method				
	U_s	t_i	h_i	t_o	h_o	U_{stA}	t_i	h_i	t_o	h_o
2.30 (0.41)	15.20 (59.4)	15.25 (2.69)	-14.59 (5.74)	25.03 (4.41)	2.11 (0.37)	20.09 (68.2)	15.19 (2.67)	-18.02 (-0.4)	27.05 (4.76)	1.92 (0.34)

4.7.3 U-factor Simulation

The simulation models used to represent Specimen #7, and the resulting component and area-weighted U-factors, are shown in Appendix G. The initial simulation produced a U-factor of 3.31 W/m²-K (0.58 BTU/hr-ft²-°F), much higher than the tested values (U_s or U_{st}), which indicates that the simulation model was accounting for far too much heat transfer in the test specimen.

The cross-sections used to represent Specimen #7, and resulting component and area-weighted U-factors, are shown in Appendix G. The initial simulation produced a total-product U-factor of 3.31 W/m²-K (0.58 BTU/hr-ft²-°F), much higher than the tested values (U_s or U_{st}), which indicated that the simulation model was accounting for far too much heat transfer in the test specimen.

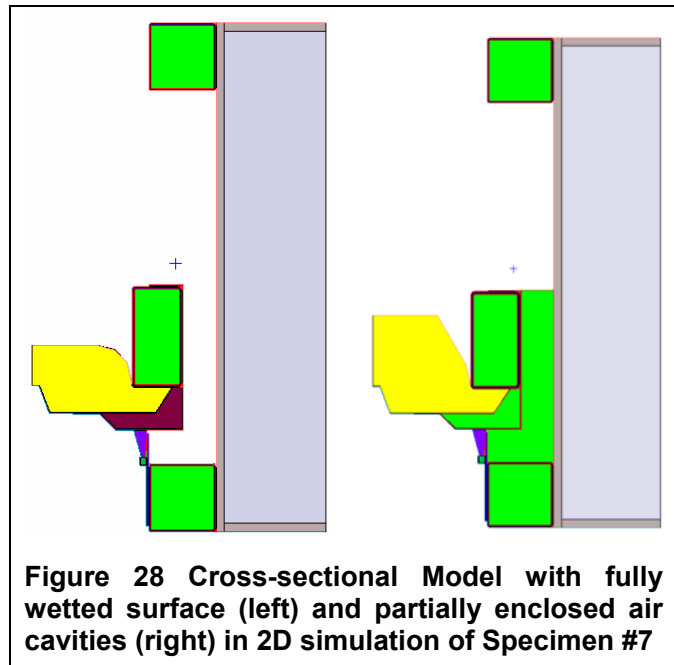


Figure 28 Cross-sectional Model with fully wetted surface (left) and partially enclosed air cavities (right) in 2D simulation of Specimen #7

At several cross-sections, the weatherstripping provided the only separation between the interior and exterior chambers in the hot box (shown at left in Figure 28). In terms of heat transfer, the significant element of thermal resistance (i.e., the “controlling resistance”) was the room-side film coefficient. Therefore, the room-side film coefficient was suspected as a source of error for the simulation model. Also, the design drawings provided by the manufacturer indicated a center-of-panel thickness of 100 mm (4”) for the batts, but field measurement of the specimen indicated that the actual thickness was 150 mm (6”).

The room-side film coefficient was adjusted in a manner similar to that for Specimen #5, as shown at right in Figure 28. Also, the thickness of the batt insulation was adjusted to match the measured value of the test specimen. With these adjustments, the simulation total-product U-factor was 2.27 W/m²-K (0.40 BTU/hr-ft²-°F). This is 7% higher than the area-weighted test result, and 15.4% higher than the CTS test result. The area-weighting method is preferred in ASTM C1199 (see Section 4.5.2), so simulation appears to provide an accurate representation of the thermal performance of the rolling hangar door.

The simulation method used in this project appears to provide an accurate representation of thermal performance for the rolling aircraft hangar / warehouse door. The method of partially enclosed air cavities (see Figure 28) is recommended.

5. EXPANSION OF SIMULATION RESULTS

Table 15 summarizes the results for all seven specimens. NFRC 100 describes “equivalence” as agreement of the U-factors from test and simulation to within 10% of the simulation value. As already noted, results for Specimens #1 and #5 do not achieve “equivalence”. Table 15 shows that, when the standardization methods recommended in ASTM C1199 are used, all other specimens achieve equivalence. Therefore, the baseline models for those specimens can be used to expand the scope of the project, by using simulation to generate an expanded table of design U-factors.

Table 15 Summary of Test and Simulation Results

Specimen	Air test, L/s per m ² (cfm/ft ²)	U-factor simulated, W/m ² °C (BTU/hr-ft ² -°F)	U-factor test, W/m ² °C (BTU/hr-ft ² -°F)	Test – Simulation Agreement (%)
1 (Non-insulated Sectional)	2.64 (0.52)	6.72 (1.18) ^C	U _s = 6.23 (1.10) U_{st} = 5.43 (0.96)^A U _{st} = 4.94 (0.87) ^B	-19.2^A -26.4 ^B
2 (Insulated Sectional)	0.85 (0.17)	1.59 (0.28) ^D	U _s = 1.60 (0.28) U _{st} = 1.45 (0.26) ^A U_{st} = 1.51 (0.27)^B	-8.8 ^A -5.0^B
3 (Three-wing Revolving)	28.7 - 83.9 (5.6 - 16.5)	4.53 (0.80)	U _s = 5.75 (1.01) U_{st} = 4.66 (0.82)^A U _{st} = 3.67 (0.65) ^B	+2.9^A -19.0 ^B
4 (Four-wing Revolving)	8.9 - 26.3 (1.75 - 5.18)	3.63 (0.64)	U _s = 4.10 (0.72) U_{st} = 3.48 (0.61)^A U _{st} = 2.93 (0.52) ^B	-4.1^A -19.3 ^B
5 (Metal Coiling Slat)	22.4 (4.41)	7.94 (1.40) ^E	U _s = 5.88 (1.04) U_{st} = 5.54 (0.98)^A U _{st} = 4.68 (0.82) ^B	-33.4^A -41.1 ^B
6 (Emergency Exit)	3.95-10.6 (0.78-2.08)	3.04 (0.53) ^C	U _s = 3.50 (0.62) U_{st} = 3.11 (0.55)^A U _{st} = 2.96 (0.52) ^B	+2.3^A -2.6 ^B
7 (Hangar/Warehouse)	10.21 (2.01)	2.27 (0.40) ^E	U _s = 2.30 (0.41) U_{st} = 2.11 (0.37)^A U _{st} = 1.92 (0.34) ^B	-7.0^A -15.4 ^B

- NOTES: ^A Test Method A = area-weighting procedure
^B Test Method B = CTS calibration procedure
^C Represents a variance from standard NFRC approach (increased edge region)
^D Represents a variance from NFRC approach (standard edge-frame area-weighting)
^E Represents a variance from NFRC approach (less exposed surface area on room side)

Results in **boldface type** indicate the preferred method of standardizing results according to ASTM C1199

5.1 ONE-PIECE AND SECTIONAL TILT-UP GARAGE DOORS

One-piece garage doors are described in Section 2.1 of this report; sectional garage doors described in Section 2.2, and are similar to Specimens #1 and #2. Typical U-factors for these product types were determined using computer simulation. Values for insulated sectional doors were generated with the base models used for Specimen #2, with different insulation used in the cross-sectional models. Non-insulated products are not included, as we did not achieve “equivalence” for Specimen #1.

The component U-factors of the resulting cross-sectional models were area-weighted following NFRC 100 to produce total-door U-factors for each product. The sizes chosen were typical of single- and double-wide one-piece garage doors (double-width sectional doors are not common: a multi-vehicle garage usually has a separate sectional door for each vehicle bay). The values for sectional garage doors represent typical products, which have four panels at the 2.13-meter (7-foot) height that is most common for residential applications.

The most common insulation options for tilt-up garage doors are prefabricated inserts of either expanded polystyrene (EPS) foam or extruded polystyrene (XPS) foam. The doors have steel skins on either side of the insulated core; some products incorporate a thermal break between the interior and exterior skins, but the thermal break design is minimal (see Figure 13). Also, one-piece doors are typically stiffened with steel ribs that run the entire width of the product, which introduces thermal bridges wherever the ribs are located, so the effect of the thermal break is small. We would encourage the development of a design incorporating a more substantial thermal break, but recognize the inherent difficulty in manufacturing a panelized product that will maintain the required stiffness and strength at the large sizes required for garages. Sectional garage doors usually do not have steel ribs, as the joints between adjacent panels provide sufficient stiffness to prevent warping.

Typical door thicknesses range from 35 mm (1 3/8”) to 100 mm (4”). We have included a theoretical door of 150 mm (6”) thickness to provide an upper end for design considerations, and because such a door could be built, if such an application were required. We would recommend that the design of the thermal break should be improved before such a door is created, however, as the thermal bridging at the stiffening ribs (in one-piece doors) and the small thermal breaks would negate much of the thermal resistance of the insulation.

Table 16 lists recommended U-factors for one-piece tilt-up garage doors, to be included in the ASHRAE Handbook of Fundamentals. Table 17 provides similar values for sectional garage doors. If desired (for example, to save space), the values for thermally broken products could be tabulated, with a footnote included to increase the U-factor by 2% in the case of products with no thermal break.

Table 16 Design U-factors for One-piece Tilt-up Garage Doors

Product Type	Size (W x H), m x m (ft x ft)	Product configuration	U-factor, W/m ² °C (BTU/hr-ft ² -°F)
35mm (1 3/8") thickness, double-skin thermally broken steel door	2.44 x 2.13 (8 x 7)	EPS insulation, steel ribs	2.03 (0.36)
		XPS insulation, steel ribs	1.86 (0.33)
	4.88 x 2.13 (16 x 7)	EPS insulation, steel ribs	1.87 (0.33)
		XPS insulation, steel ribs	1.70 (0.30)
50 mm (2") thickness, double- skin thermally broken steel door	2.44 x 2.13 (8 x 7)	EPS insulation, steel ribs	1.71 (0.30)
		XPS insulation, steel ribs	1.59 (0.28)
	4.88 x 2.13 (16 x 7)	EPS insulation, steel ribs	1.55 (0.27)
		XPS insulation, steel ribs	1.42 (0.25)
76 mm (3") thickness, double- skin thermally broken steel door	2.44 x 2.13 (8 x 7)	EPS insulation, steel ribs	1.43 (0.25)
		XPS insulation, steel ribs	1.35 (0.24)
	4.88 x 2.13 (16 x 7)	EPS insulation, steel ribs	1.27 (0.22)
		XPS insulation, steel ribs	1.18 (0.21)
102 mm (4") thickness, double- skin thermally broken steel door	2.44 x 2.13 (8 x 7)	EPS insulation, steel ribs	1.27 (0.22)
		XPS insulation, steel ribs	1.21 (0.21)
	4.88 x 2.13 (16 x 7)	EPS insulation, steel ribs	1.11 (0.20)
		XPS insulation, steel ribs	1.04 (0.18)
152 (6") thickness, double-skin thermally broken steel door	2.44 x 2.13 (8 x 7)	EPS insulation, steel ribs	1.09 (0.19)
		XPS insulation, steel ribs	1.05 (0.18)
	4.88 x 2.13 (16 x 7)	EPS insulation, steel ribs	0.92 (0.16)
		XPS insulation, steel ribs	0.87 (0.15)
35mm (1 3/8") thickness, double-skin thermally unbroken steel door	2.44 x 2.13 (8 x 7)	EPS insulation, steel ribs	2.06 (0.36)
		XPS insulation, steel ribs	1.90 (0.33)
	4.88 x 2.13 (16 x 7)	EPS insulation, steel ribs	1.90 (0.33)
		XPS insulation, steel ribs	1.74 (0.31)
50 mm (2") thickness, double- skin thermally unbroken steel door	2.44 x 2.13 (8 x 7)	EPS insulation, steel ribs	1.74 (0.31)
		XPS insulation, steel ribs	1.62 (0.29)
	4.88 x 2.13 (16 x 7)	EPS insulation, steel ribs	1.58 (0.28)
		XPS insulation, steel ribs	1.46 (0.26)
76 mm (3") thickness, double- skin thermally unbroken steel door	2.44 x 2.13 (8 x 7)	EPS insulation, steel ribs	1.46 (0.26)
		XPS insulation, steel ribs	1.37 (0.24)
	4.88 x 2.13 (16 x 7)	EPS insulation, steel ribs	1.29 (0.23)
		XPS insulation, steel ribs	1.21 (0.21)
102 mm (4") thickness, double- skin thermally unbroken steel door	2.44 x 2.13 (8 x 7)	EPS insulation, steel ribs	1.29 (0.23)
		XPS insulation, steel ribs	1.22 (0.21)
	4.88 x 2.13 (16 x 7)	EPS insulation, steel ribs	1.13 (0.20)
		XPS insulation, steel ribs	1.06 (0.19)
152 (6") thickness, double-skin thermally unbroken steel door	2.44 x 2.13 (8 x 7)	EPS insulation, steel ribs	1.11 (0.20)
		XPS insulation, steel ribs	1.06 (0.19)
	4.88 x 2.13 (16 x 7)	EPS insulation, steel ribs	0.93 (0.16)
		XPS insulation, steel ribs	0.88 (0.15)

Table 17 Design U-factors for Sectional Tilt-up Garage Doors

Product Type	Size (W x H), m x m (ft x ft)	Product configuration	U-factor, W/m ² °C (BTU/hr-ft ² -°F)
35mm (1 3/8") thick, double-skin thermally broken steel door	2.74 x 2.13 (9 x 7)	EPS insulation, steel ribs	1.94 (0.34)
		XPS insulation, steel ribs	1.76 (0.31)
50 mm (2") thick, double-skin thermally broken steel door	2.74 x 2.13 (9 x 7)	EPS insulation, steel ribs	1.66 (0.29)
		XPS insulation, steel ribs	1.53 (0.27)
76 mm (3") thick, double-skin thermally broken steel door	2.74 x 2.13 (9 x 7)	EPS insulation, steel ribs	1.43 (0.25)
		XPS insulation, steel ribs	1.34 (0.24)
102 mm (4") thick, double-skin thermally broken steel door	2.74 x 2.13 (9 x 7)	EPS insulation, steel ribs	1.29 (0.23)
		XPS insulation, steel ribs	1.22 (0.21)
152 mm (6") thick, double-skin thermally broken steel door	2.74 x 2.13 (9 x 7)	EPS insulation, steel ribs	1.13 (0.20)
		XPS insulation, steel ribs	1.08 (0.19)
35mm (1 3/8") thick, double-skin thermally broken steel door	2.74 x 2.13 (9 x 7)	EPS insulation, steel ribs	2.19 (0.39)
		XPS insulation, steel ribs	2.05 (0.36)
50 mm (2") thick, double-skin thermally broken steel door	2.74 x 2.13 (9 x 7)	EPS insulation, steel ribs	1.87 (0.33)
		XPS insulation, steel ribs	1.77 (0.31)
76 mm (3") thick, double-skin thermally broken steel door	2.74 x 2.13 (9 x 7)	EPS insulation, steel ribs	1.60 (0.28)
		XPS insulation, steel ribs	1.52 (0.27)
102 mm (4") thick, double-skin thermally broken steel door	2.74 x 2.13 (9 x 7)	EPS insulation, steel ribs	1.43 (0.25)
		XPS insulation, steel ribs	1.36 (0.24)
152 mm (6") thick, double-skin thermally broken steel door	2.74 x 2.13 (9 x 7)	EPS insulation, steel ribs	1.22 (0.21)
		XPS insulation, steel ribs	1.17 (0.21)

5.2 REVOLVING DOORS

As noted in Sections 4.3 and 4.4, the procedure used to develop U-factors for the revolving doors in this project is quite experimental. The project was successful, in that we developed methodologies for testing and simulating U-factors of revolving doors, but we do not recommend expanding the scope of results for these products until more validation can be done in subsequent research. The extent of extrapolation appropriate for the products evaluated here would permit generating U-factors at different sizes than those tested, but anything beyond that would be excessive. The recommended values to be included in the Handbook of Fundamentals are listed in Table 18.

Table 18 Design U-factors for Revolving Doors

	Size (W x H), m x m (ft x ft)	U-factor, W/m ² °C (BTU/hr-ft ² -°F)
3-wing revolving door	2.44 x 2.13 (8 x 7)	4.46 (0.79)
	3.28 x 2.44 (10 x 8)	4.53 (0.80)
4-wing revolving door	2.13 x 1.98 (7 x 6.5)	3.56 (0.63)
	2.13 x 2.29 (7 x 7.5)	3.63 (0.64)

5.3 EMERGENCY EXIT DOORS

Emergency exit doors are described in Section 2.5 of this report, and are similar to Specimen #6. Typical U-factors for these product types were generated with the base models used for Specimen #6, with different insulation used in the cross-sectional models.

The component U-factors of the resulting cross-sectional models were area-weighted following NFRC 100 to produce total-door U-factors for each product. The sizes chosen were typical of single- and double-door assemblies, with a simple astragal included between the door slabs in the double-door models.

The most common insulation options for emergency exit doors are honeycombed kraft paper, mineral wool, or expanded polyurethane foam. The doors have steel skins on either side of the insulated core; some products incorporate a thermal break between the interior and exterior skins, but the thermal break design is minimal. Also, doors insulated with mineral wool are typically stiffened with steel ribs that run the width of the product, so the effect of the thermal break is reduced. Typical door thicknesses are 35 mm (1 3/8") or 45 mm (1 3/4").

Table 19 lists recommended U-factors for emergency exit doors, to be included in the ASHRAE Handbook of Fundamentals.

Table 19 Design U-factors for Emergency Exit Doors

Product Type	Size (W x H), m x m (ft x ft)	Core insulation	U-factor, W/m ² °C (BTU/hr-ft ² -°F)
35 mm (1 3/8") thickness, double-skin thermally broken steel door	0.91 x 2.03 (3 x 6'8")	honeycomb kraft paper	3.23 (0.57)
		mineral wool, steel ribs	2.50 (0.44)
		polyurethane foam	1.92 (0.34)
	0.91 x 2.03 (6 x 6'8")	honeycomb kraft paper	2.97 (0.52)
		mineral wool, steel ribs	2.05 (0.36)
		polyurethane foam	1.60 (0.28)
44 mm (1 3/4") thickness, double-skin thermally broken steel door	0.91 x 2.03 (3 x 6'8")	honeycomb kraft paper	3.25 (0.57)
		mineral wool, steel ribs	2.30 (0.41)
		polyurethane foam	1.77 (0.31)
	0.91 x 2.03 (6 x 6'8")	honeycomb kraft paper	3.06 (0.54)
		mineral wool, steel ribs	1.90 (0.33)
		polyurethane foam	1.50 (0.26)
35 mm (1 3/8") thickness, double-skin steel door (no thermal break)	0.91 x 2.03 (3 x 6'8")	honeycomb kraft paper	3.38 (0.60)
		mineral wool, steel ribs	2.67 (0.47)
		polyurethane foam	2.10 (0.37)
	0.91 x 2.03 (6 x 6'8")	honeycomb kraft paper	3.11 (0.55)
		mineral wool, steel ribs	2.21 (0.39)
		polyurethane foam	1.77 (0.31)
44 mm (1 3/4") thickness, double-skin steel door (no thermal break)	0.91 x 2.03 (3 x 6'8")	honeycomb kraft paper	3.38 (0.60)
		mineral wool, steel ribs	2.47 (0.44)
		polyurethane foam	1.95 (0.34)
	0.91 x 2.03 (6 x 6'8")	honeycomb kraft paper	3.22 (0.57)
		mineral wool, steel ribs	2.08 (0.37)
		polyurethane foam	1.69 (0.30)

5.4 AIRCRAFT HANGAR DOORS

Hangar doors are described in Section 2.6 of this report, and are similar in design to Specimen #7. Typical U-factors for these product types were generated with the base models used for Specimen #7, with different insulation used in the cross-sectional models.

The component U-factors of the resulting cross-sectional models were area-weighted following NFRC 100 to produce total-door U-factors for each product. The as-tested size of Specimen #7, 3245 mm x 3245 mm (128" x 128"), is not representative of typical hangar doors, which would not fit into a commercial test facility. A typical aircraft hangar door for a small single-engine aircraft such as a Cessna Skyhawk 172 is approximately 22 m x 3.7m (72' x 12'), whereas a hangar suitable for a typical commercial jet (Boeing 737 or Airbus A320) should be at least 73 m x 15.2 m (240' x 50'). Ideally, the aspect ratio of the door panels is kept close to 1.0 to avoid binding the roller mechanism, which means that the large and small hangar doors both have four moving panels (two one either side of an astragal) and two stationary panels (one on each side: the moving panels roll behind the stationary panels for storage). Other configurations are possible, and these doors are often custom-manufactured, so the values listed here should not be considered as definitive. Door thicknesses chosen to generate design U-factors reflect typical 38 mm x 89 mm (nominal 2" x 4") and 38 mm x 140 mm (nominal 2" x 6") frame construction.

Rolling hangar doors are typically constructed similar to wall panels mounted on a rolling track, so a large number of insulation options are available. We have chosen three typical insulation materials (EPS, XPS and mineral wool or glass-fiber batts), and have included a non-insulated option. Where a door is insulated with mineral wool or glass-fibre batts, the insulation is draped on the inner surface, just like the test specimen (see Figure 27). Where rigid insulation is used, the insulation boards are typically in 600 mm (2') widths, so Z-girts can be used to hold the insulation in place. Although more energy-conscious manufacturers might use fasteners with large heads to fasten the rigid insulation in place and minimize thermal bridging, these doors are typically not manufactured with energy efficiency in mind. The products with rigid insulation represented in Table 20 feature horizontal Z-girts spaced at 600 mm (2') on center.

Table 20 Design U-factors for Aircraft Hangar Doors

Product Type	Size (W x H), m x m (ft x ft)	Core insulation	U-factor, W/m ² ·C (BTU/hr·ft ² ·°F)
38 mm x 89 mm (nominal 2"x4") steel-frame construction rolling hangar door	21.9 x 3.7 (72 x 12)	non-insulated	6.27 (1.10)
		expanded polystyrene	1.40 (0.25)
		mineral wool, steel ribs	1.45 (0.25)
		extruded polystyrene	1.32 (0.23)
	73 x 15.2 (240 x 50)	non-insulated	7.00 (1.23)
		expanded polystyrene	0.91 (0.16)
		mineral wool, steel ribs	0.92 (0.16)
		extruded polystyrene	0.83 (0.15)
38 mm x 140 mm (nominal 2"x6") steel-frame construction rolling hangar door	21.9 x 3.7 (72 x 12)	non-insulated	6.27 (1.10)
		expanded polystyrene	1.18 (0.21)
		mineral wool, steel ribs	1.28 (0.23)
		extruded polystyrene	1.14 (0.20)
	73 x 15.2 (240 x 50)	non-insulated	7.00 (1.23)
		expanded polystyrene	0.72 (0.13)
		mineral wool, steel ribs	0.73 (0.13)
		extruded polystyrene	0.67 (0.12)

6. CONCLUSIONS AND RECOMMENDATIONS

The following recommendations are collected from throughout the report.

- #1) ASTM C1199 should be followed regarding area-weighting vs. CTS methods for high-conductance specimens ($U_s > 3.4 \text{ W/m}^2\text{-K}$ or $0.6 \text{ BTU/hr-ft}^2\text{-}^\circ\text{F}$) and for projecting products ($A_p \ll A_s$).**

Specific Standards Language: NFRC 102 contains a clause (Clause 8.2) that modifies ASTM C1199 to require the CTS method to be used for all products. This does not appear to be appropriate for high-conductance products or projecting products, and we recommend that this clause be removed from NFRC 102.

- #1a) Clause 8.2 in NFRC 102 should be deleted.**

- #2) A larger portion of edge-of-panel should be included in the 2D model for steel-skin garage doors and emergency exit doors. It requires little additional effort to create the model, and greatly improves the accuracy of the result.**

Specific Standards Language: where Figures 5-2a and 5-2b in NFRC 100-2004 indicates that the edge-of-panel area for steel-skin swinging entrance doors is 63.5 mm (2.5"), this should be changed to the 150 mm (6") dimension developed in this study, but there is no guarantee that this would be suitable for all products.

The technically correct methodology, as was used in this project, is to incrementally increase the edge-of-panel height until subsequent iterations produce no change in the result, but this may not be desirable language in a Standard such as NFRC 100.

This argument also applies to Figure 5-13 in NFRC 100-2004, which refers to garage doors.

- #2a) Figures 5-2a, 5-2b and 5-13 in NFRC 100 should be modified so that the "edge-of-panel area" reads 150 mm (6") instead of 63.5 mm (2.5") – or so that it reads "Edge-of-Panel Area: height varies", with a direction in the NFRC Simulation Manual to incrementally increase edge-of-panel height until subsequent iterations produce no change in the result.**

- #3) The NFRC 102 Standard should clarify whether the emittance of the specimen is to be measured procedure, or if standardized values are to be used.**

Specific Standards Language: NFRC 101 provides a method for measuring surface emittance, and also provides default values for many types of surfaces. Clause 6.5.2.2(A).a of NFRC 102 specifies that the tape used to hold thermocouples in place should be similar to the specimen, but as the emittance of the specimen is not known at this point, the requirement to measure the emittance (or use a default value) should be specified before this Clause. Our preference would be to use the default values in Appendix A of NFRC 101, to ensure a more standardized approach, but measured values should always be permitted in lieu of the default values.

- #4) The THERM program should be modified to allow users to input actual specimen height.**

- #5) Methods used to determine film coefficients in test and computer-simulation procedures should be studied further, to develop a method that provides consistent results. Alternatively, equation <3> (from Clause 8.2.9.1 in NFRC 102) could be programmed into the software, which would then solve for T_{is} and adjust h_{STH} accordingly to achieve an iterative solution. The original approach allowed the user to specify a standardized film coefficient in the software, and this seemed to work reasonably well.**

- #6) It appears that a pressure-balanced test protocol is not sufficient to eliminate the effects of air leakage in a thermal test. We therefore recommend that test procedures for thermal transmittance should always require sealing against air leakage.**

Specific Standards Language: the above recommendation is in keeping with NFRC procedures.

- #7) A large test specimen with a reasonably low thermal transmittance may exhibit significant deflection when subjected to a large temperature difference. We therefore recommend that such products should be sealed against air leakage in such a manner that anticipates some movement as a result of this deflection, and maintains the air seal for the duration of the test. This deflection should also be kept in mind when calculating the heating, cooling and ventilation loads for a building during the design stage.**

Specific Standards Language: Clause 5.1.5(A) of NFRC 102 could be modified by adding the sentence: "For large specimens (i.e., above 2m x 2m), the seal should be constructed so as to anticipate movement of the specimen due to thermal stresses."

- #8) The simulation and test methods used in this project do not appear to provide an accurate representation of thermal performance for the non-insulated sectional garage door or the non-insulated metal coiling slat door. We do not recommend using computer simulation to expand the scope of products represented in the design tables of the Handbook of Fundamentals for this project.**

- #9) The modified simulation and test methods used in this project appear to provide an accurate representation of thermal performance for the insulated sectional garage door, emergency exit door, and aircraft hangar door. We recommend using computer simulation to expand the scope of products represented in the design tables of the Handbook of Fundamentals for this project.**

- #9a) The automatic use of a fully wetted surface, as shown in Figure 25, should be reviewed to ensure that it does not produce unrealistic models in the case of complex articulated surfaces (e.g., metal coiling slat doors). Also, in the case of partially enclosed cavities created by roller tracks, the method of partially enclosed air cavities (see Figure 28) is recommended.**

- #10) The simulation method used in this project appears to provide an accurate representation of thermal performance for the 3-wing and 4-wing revolving doors. The area-weighting method of standardizing test results also appears to provide good agreement with simulation for this case. As this procedure is experimental, however, we do not recommend its use in expanding the scope of results for this project until more validation can be done on these types of products in subsequent research.**

- #11) Tables 16 through 20 should be included in the ASHRAE Handbook of Fundamentals, to provide design U-factors for garage doors, emergency exit doors, and rolling warehouse and aircraft-hangar doors.**

- #12) The air-leakage equations presented in this report should be considered for inclusion in the ASHRAE Handbook of Fundamentals, as they provide some guidelines for air-leakage characteristics of the products investigated in this study.**

REFERENCES

- ASHRAE, 2001a. Handbook of Fundamentals. 2004, American Society for Heating, Refrigerating and Air-Conditioning Engineers, Inc., Atlanta, GA
- ASTM, 2000. C1199-00: Standard test method for measuring the steady-state thermal transmittance of fenestration systems using hot box methods. 2000, ASTM International, West Conshohocken, PA.
- Enermodal, 1996. Procedures for modeling the energy performance of building components: doors and walls. 1996, Enermodal Engineering Ltd., Kitchener, ON.
- ISO, 2002. UISO/FDIS 15099: Thermal performance of windows, doors and shading devices – detailed calculations. 2002, ISO Central Secretariat, Geneva, Switzerland.
- LBNL, 2003. THERM 5.2: A PC program for analyzing two-dimensional heat transfer through building products. 2003, Regents of the University of California, Berkeley, CA.
- NFRC, 2004a. NFRC100-2004: Procedure for determining fenestration product U-factors. 2004, National Fenestration Rating Council, Silver Spring, MD.
- NFRC, 2004b. NFRC 101-2004: Procedure for determining thermophysical properties for use in NFRC-approved software programs. 2004, National Fenestration Rating Council, Silver Spring, MD.
- NFRC, 2004c. NFRC 102-2004: Procedure for measuring the steady-state thermal transmittance of fenestration systems. 2004, National Fenestration Rating Council, Silver Spring, MD.
- NFRC, 2004d. NFRC 400-2004: Procedure for determining fenestration product air leakage. 2004, National Fenestration Rating Council, Silver Spring, MD.